







# **Ana Laura Veiga Nunes**

Degree in Biochemistry

# Studies of the RIC protein in Staphylococcus aureus

Dissertation to obtain the Master Degree in Biochemistry for Health

Supervisor: Professor Lígia Saraiva, ITQB-NOVA





## **Ana Laura Veiga Nunes**

Degree in Biochemistry

## Studies of the RIC protein in Staphylococcus aureus

Dissertation to obtain the Master degree in Biochemistry for Health

Supervisor: Professor Lígia Saraiva

Juri:

President: Doctor Pedro Matias

Opponent: Doctor Filipe dos Santos Folgosa

Supervisor: Professor Lígia Saraiva

Instituto de Tecnologia Química e Biológica, António Xavier

March, 2021

## Studies of the RIC protein in Staphylococcus aureus

## Copyright

O Instituto de Tecnologia Química e Biológica António Xavier e a Universidade Nova de Lisboa têm o direito, perpétuo e sem limites geográficos, de arquivar e publicar esta dissertação através de exemplares impressos reproduzidos em papel ou de forma digital, ou por qualquer outro meio conhecido ou que venha a ser inventado, e de a divulgar através de repositórios científicos e de admitir a sua cópia e distribuição com objetivos educacionais ou de investigação, não comerciais, desde que seja dado crédito ao autor e editor.

## **Agradecimentos**

Gostaria de expressar a minha gratidão à minha orientadora, a Professora Doutora Lígia Saraiva, por todos os conselhos, ensinamentos, partilha de conhecimento e tempo disponibilizado.

Um agradecimento também à minha "coorientadora" futura doutora Liliana Silva que teve o carinho paciência e dedicação para me ensinar as coisas tanto a nível teórico como a nível prático, acho que não seria qualquer pessoa que teria feito por mim o que a Liliana fez.

A todos os colegas do laboratório, nomeadamente ao Marco, à Claúdia, à Joana, à Sofia, à Sandra e ao Jordi, gostaria de agradecer a maneira graciosa que me receberam, por toda a ajuda prestada, todos os conselhos que me deram para o meu desenvolvimento.

Agradeço também aos meus colegas de mestrado, um obrigado ao Gonçalo, à Salomé, à Rita, à Jéssica e à Ana que me fizeram companhia nas pequenas pausas de descontração. À minha família, em especial à mais próxima, um por todo o apoio que me transmitiram e por me permitirem dedicar a tempo inteiro ao meu curso e darem-me a oportunidade de seguir o meu sonho.

À Mónica Cardoso, agradeço do fundo coração de estar comigo desde o início deste meu percurso, que sempre esteve lá para mim nos tempos bons como também nos mais difíceis.

Ao Kiko, agradeço por teres sido o meu melhor amigo, estiveste comigo em todos os momentos bons, maus, assim assim e sabias sempre o que se passava comigo. Obrigada por me teres tornado numa melhor pessoa. Amo-te ontem hoje e sempre.

### **Abstract**

Repair Iron center (RIC) protein is a di-iron center containing protein widely distributed among bacteria that contributes to pathogen resistance. In *Escherichia coli*, RIC is able to donate iron for repairing of damaged iron sulfur clusters. Moreover, RIC protein confer resistance to *Staphylococcus aureus* exposed to reactive oxidative and nitrosative stresses in murine macrophages.

In this thesis, the RIC protein of S. aureus JE2, a MRSA strain was studied.

I started by evaluate and compare the viability of *S. aureus* JE2 wild type and JE2 *ric* mutant, with that of *E. coli katE*, *katG* and *katEG* mutant strain when exposed to oxidative stress conditions. The results showed that all strains had its growth impaired under these conditions.

Next, I determined the catalase activity of cell extracts of the *S. aureus ric* mutant. Strains of JE2 wild type and JE2 $\Delta$ *ric* were exposed to H<sub>2</sub>O<sub>2</sub> and the catalase activity of cell extracts collected at defined times was determined. The results showed a decrease in the catalase activity of the mutant by ~70% for cells harvested at the exponential phase, and of ~ 10% for cells collected at the stationary phase, The catalase activity of JE2 $\Delta$ *ric* complemented, separately, with two plasmids expressing RIC in trans (pMK4RIC and pspcapMK4RIC) was also evaluated. Data showed that only the mutant cells complemented with pspcapMK4RIC restored the wild type phenotype.

The catalase activity of the purified RIC protein was also evaluated. The results of the enzymatic activity of the purified S. aureus RIC protein indicated that RIC has catalase activity with  $V_m$  and  $K_m$  values of 30.35 mmol / (min mg<sub>protein</sub>) and 15.94 mM, respectively.

I also studied the interaction of *S. aureus* RIC with *S. aureus* DNA-binding protein from starved cells (Dps), and obtained results showing that the two proteins interact, a study that needs to be further explored.

Altogether, the results show an important role for *S. aureus* RIC protein in bacterial protection from the oxidative stress imposed by the innate immune system.

Resumo

A proteína RIC, presente em diversas bactérias, confere resistência a patógenos. Esta

proteína contém um centro di-ferro e, em Escherichia coli, esta tem como função doar ferro para a

reparação de centros de ferro enxofre danificados. Adicionalmente, a proteína RIC confere

resistência ao stress oxidativo e nitrosativo aquando da bactéria Staphylococcus aureus é fagocitada

por macrófagos.

Nesta dissertação, realizou-se o estudo da proteína RIC da estirpe JE2 de S. aureus,

Inicialmente, comecei por avaliar e comparar a viabilidade celular, em condições de stress

oxidativo, das células JE2 e respetivo mutante de ric de S, aureus, com a viabilidade das células de

E. coli e respetivos mutantes de catálase (katE, katG e katEG). Os resultados demostraram que

todas as estirpes, nestas condições, tiveram seu crescimento afetado.

Em seguida, determinei a atividade de catálase de extratos celulares de JE2 e respetivo

mutante de ric. Nestes ensaios, recolheram-se vários extratos correspondendo a diferentes fases do

crescimento e a atividade de catálase foi determinada utilizando H<sub>2</sub>O<sub>2</sub> como substrato. Os resultados

mostraram uma diminuição de ~70% e de ~ 10% na atividade da catálase do mutante em células

colhidas na fase exponencial e na fase estacionária, respetivamente. Também foi avaliada a

atividade da catálase do mutante JE2\(\Delta ric\) complementado, separadamente, com dois plasmídeos

que expressam RIC (pMK4RIC e pspcapMK4RIC). Os dados obtidos indicam que as células

mutantes complementadas com pspcapMK4RIC restauraram o fenótipo do wild type.

Avaliou-se a atividade de catálase da proteína RIC purificada. Os resultados da atividade

enzimática da proteína RIC de S. aureus purificada indicam que a RIC possui atividade catálase com

valores de V<sub>m</sub> e K<sub>m</sub> de 30.35 mmol / (min mg<sub>proteína</sub>) e 15.94 mM, respetivamente.

Estudei também a interação da proteína RIC e Dps de S. aureus. Os resultados obtidos

demonstram que estas proteínas interagem.

Em conjunto, os resultados mostram a importância da proteína RIC de S. aureus na proteção

bacteriana contra o stress oxidativo imposto pelo sistema imune inato.

Palavras-chave: S. aureus, proteína di ferro RIC, stress oxidativo, catálase

VII

# Index

1.	Introduction	1
	1.1 Staphylococcus aureus	1
	1.2. Iron sulfur clusters	3
	1.3. Repair Iron Centers Protein	4
2.	Aims and motivations	7
3.	Material and Methods	9
	3.1. Strain Complementation	9
	3.1.1. DNA extraction	9
	3.1.2. Strain Transformation	. 10
	3.2. DNA Cloning	. 12
	3.3. Protein purification	. 12
	3.3.1. Protein Expression	. 12
	3.3.2. Protein Purification	. 12
	3.4. Oxidative stress assays	. 13
	3.5. Viability assays	. 14
	3.6. Enzymatic assays	. 14
	3.6.1. Catalase activity assays	. 15
	3.7. Protein quantification of cell extracts and purified protein	. 16
	3.8. Iron Quantification	. 17
	3.9. Protein-protein interaction studies	. 17
	3.10. Site-Directed Mutagenesis	. 18
4.	Results and Discussion	. 21
	4.1. Oxidative stress resistance and viability assays	. 21
	4.2. Enzymatic activity assays	. 23
	4.2.1. Catalase activity in cell extracts	. 23
	4.2.2. Catalase activity with purified RIC protein	. 30
	4.3. Catalase complementation	. 34

	4.4. Protein-Protein interactions	38
	4.5. Site-directed mutagenesis	. 40
5.	Conclusions	. 43
6.	References	45
S	. Supplements	. 49

# Index of figures

_		different types of [2Fe-2		_	_			•	•
Figure	1.2	- Homology-based	modelling	of	the	E.	coli	RIC	structure
Figure 4	<b>l.1</b> - Rep	resentation of the grow	th curves JE	2 and	JE2Δ <i>r</i>	<i>ic</i> stra	ins in t	he oxid	ative stress
Figure 4	. <b>2</b> - Repr	esentation of JE2 e JE2	∆ <i>ric</i> cell viabi	lity					22
Figure 4	<b>.3</b> - Repre	esentation of the enzyma	atic activity of	JE2 e	JE2∆ <i>ri</i>	c extra	icts		24
_	•	esentation of the enzyn	-						
Figure 4	. <b>5</b> - Enzy	matic activity of <i>E. coli</i> k	K12ATCC and	d K12/	∆ <i>ric</i>				26
_		resentation of enzymat	-		_				
_		rmination of the enzyma	-					-	
_	-	matic activity of the JE2 until an OD of 3			-				
_		matogram obtained in the column.	•					•	•
Figure 4	. <b>10</b> - Ima	ge of size exclusion chr	omatography	colum	n purif	ying th	ne RIC <sub>I</sub>	protein.	31
_		omatogram obtained in	-				-	-	
Figure 4	.12 - SDS	S-PAGE illustrating the l	RIC purification	on					33
Figure 4	. <b>13</b> – UV	-visible spectrum of the	RIC protein.						33
_		aureus RIC protein Kine				_	_		
_	•	oresentation of the grow							

<b>Figure 4.16</b> - Oxidative stress assays of E. coli BW25113 WT and mutants <i>katE, katEG</i> ar complemented strains (pMK4+RIC, pUC18+YtfE)	
<b>Figure 4.17</b> - Determination of the enzymatic activity of <i>E. coli</i> BW25113 wild type, <i>katE</i> , <i>katG</i> , <i>katE</i> mutants and complementations (pMK4-RIC pUC18-YftE) extracts using 10mM of hydrogen peroxid	le.
<b>Figure 4.18</b> - BiFC assay of the RIC interaction with Dps. The interaction forms tested were RIC <sup>N-G</sup> + DPS <sup>C-GFP</sup> and DPS <sup>N-GFP</sup> + RIC <sup>C-GFP</sup> interaction forms.	
<b>Figure 4.19</b> - Colony PCR of the strains <i>E. coli</i> XL1 and XL10 in a 1% agarose gel. 1- ladder Promeg 1Kb. 2 to 4 - single mutant AxxxE) 5 to 11 -doble mutant (GxxxE AxxxE).	-
Figure S.1. – A 1% agarose gel exemplifying and colony PCR of <i>E. coli</i> XL1	19
<b>Figure S.2</b> – Digestion of pMK4 plasmid. 1% agarose 1% gel containing the pDNA <i>S. aureus</i> RN422 digested and non-digested	
<b>Figure S.3</b> – Transformation of JE2Δ <i>ric</i> with pMK4 and pMK4-RIC for the complementation activi assays.	•
Figure S.4 – BCA calibration curve used to quantify the mg of protein present in the cell lysates are purified protein.	
Figure S.5 – TPTZ calibration curve used in the RIC protein iron quantification	51

# Index of tables

Table 3.1 - List of the bacteria and the different strains used	9
Table 3.2 - List of plasmids used for complementations. All these plasmids were study in S.	aureus
JE2Δ <i>ric</i>	10
Table 3.3 - List of plasmids used in E. coli for complementation assays	11

## List of Abbreviations

Ahp - alkyl hydroperoxide reductase

BCA - bicinchoninic acid

BSA- Bovine serum albumin

BiFC - Bimolecular fluorescence complementation

CA-MRSA - community associated MRSA

CFUs - Colony Formation Units

CHIPS - chemotaxis inhibitory protein of S. aureus

Dps - DNA-binding protein from starved cells

E. coli - Escherichia coli

Eap - extracellular adherence protein

Fe-S - Iron-Sulfur

GFP - green fluorescent protein

GOI - Gene of interest

Gpx - glutathione peroxidase

IPTG - isopropyl-β-D-thiogalactosidase

Isc - iron sulfur cluster

Kat - catalysis

LB - Luria-Bertani

MRSA - methicillin-resistant S. aureus

MSCRAMM - Microbial Surface Components Recognizing Adhesive Matrix Molecules

NADH - Nicotinamide adenine dinucleotide hydrogen

**OD - Optical density** 

PBPs - penicillin binding proteins

pDNA - plasmid DNA

PCR - Polymerase Chain Reaction

PVL - Panton-Valentine leukocidin

RIC - Repair Iron Center

RNS - reactive nitrogen species

ROS - reactive oxygen species

RT – room temperature

S. aureus - Staphylococcus aureus

Sod - superoxide dismutase

SDS – PAGE - sodium dodecyl sulphate – polyacrylamide gel electrophoresis

Suf - sulfur formation

TCA - tricarboxylic acid

Trx - thioredoxin reductase

TSB – Tryptic Soy Broth

V<sub>0</sub> - initial rate

V<sub>m</sub>- maximum velocity

WT - Wild Type

## 1. Introduction

When the human body is infected by bacteria, the innate immune system is activated triggering the action of primarily macrophages and neutrophils<sup>1</sup>. These host cells are recruited to the sites of infection to phagocyte pathogens, such as *Escherichia coli* (*E. coli*) and *Staphylococcus aureus* (*S. aureus*). During phagocytosis, antimicrobial substances are released, such as reactive oxygen species (ROS), reactive nitrogen species (RNS), proteases, and lysozyme that damage key cellular components of the pathogen, such as lipids, DNA and proteins <sup>2–4</sup>. However, bacteria have defenses against ROS and RNS, namely antioxidant enzymes (e.g. catalase, superoxide dismutase) that neutralize ROS<sup>5</sup>. Among the several system of protection against stress, several genes are activated, including the *ric* gene, which confer resistance to oxidative and nitrosative stress <sup>6,7</sup>.

ROS and RNS cause significant damage to the majority of biomolecules<sup>4,8</sup>. Among the ROS, superoxide and hydrogen peroxide primarily oxidize iron-sulfur clusters, which results in the release of iron. Iron-sulfur clusters have a redox-sensitive cofactor. Because of this, the oxidation not only damages the cofactor and inhibits enzymatic activity, but it also releases free iron that can propagate the oxidative stress<sup>4,9</sup>, in which the free iron (Fe<sup>+2</sup> and Fe<sup>+3</sup>) reacts with free radicals generating, via Fenton and Haber-Weiss reactions (1, 2) that cause cellular damage<sup>9</sup>.

$$((1) Fe^{2+} + -H_2O_2 \rightarrow Fe^{3+} + HO \cdot + OH^-$$
and

(2) 
$$Fe^{3+}+H_2O_2 \rightarrow Fe^{2+}+HOO_{+}H_{+}^{+}$$
; net =•O2-+H2O2 $\rightarrow$ •OH + OH-+O<sub>2</sub>),

### 1.1. - Staphylococcus aureus

*S. aureus* is a Gram-positive, facultative anaerobic, non-motile, asporogenous, coccal bacterium<sup>10</sup>. These bacteria are commonly found in the respiratory tract as commensals. *S. aureus* is an opportunistic pathogenic organism<sup>11</sup> that causes numerous diseases ranging from mild skin infections and soft tissues<sup>12</sup>, such as impetigo, folliculitis and cutaneous abscesses<sup>13</sup> to more severe infections including bacteremia, endocarditis, osteomyelitis and descending urinary tract infections, pyomyositis, fasciitis and pneumonia<sup>14,15</sup>.

S. aureus has become a therapeutic challenge due to its high ability to acquire resistance to multiple antibiotics, strains that in general are known as methicillin-resistant S. aureus (MRSA)

strains. The emergence of community associated MRSA (CA-MRSA) strains has increased a lot in the past few years and its prevalence in the community is resulting in high morbidity and in high mortality<sup>15–17</sup>.

MRSA strains containing the mecA gene have resistance to class  $\beta$ -lactam antibiotics such as penicillins<sup>2</sup>, cephalosporins and carbapenems, because this gene encodes a low-affinity penicillinbinding protein PBP2a<sup>16</sup>. This protein, due to its low affinity for  $\beta$ -lactams, provides a transpeptidase activity, which allows the cell wall synthesis at antibiotics concentrations that inhibit the penicillin binding proteins (PBPs), being crucial for bacteria survival<sup>18</sup>.

However, antibiotic resistance is not against on class  $\beta$ -lactam antibiotics but also to non- $\beta$ -lactam antibiotics. Resistance to sulphonamides, trimethoprim, tetracyclines, aminoglycosides, chloramphenicol, clindamycin and vancomycin<sup>19</sup>, is a concern since these antibiotics, especially vancomycin, are the main antibiotics used to treat MRSA strains nowadays<sup>4,19</sup>.

In the process of infection, *S. aureus* produces virulence factors that allow attachment, invasion and evasion in the host's immune system. These virulence factors are according to the pathogenesis and their respective virulence mechanisms<sup>17,20</sup>. During the colonization process proteins known as Microbial Surface Components Recognizing Adhesive Matrix Molecules (MSCRAMM) are secreted, promoting the adhesion of *S. aureus* to the host cells<sup>21</sup>. At initial exposure of *S. aureus* to host tissues, many upregulation virulence genes are triggered<sup>17</sup>. Depending on the site of infection, the pathogenesis of *S. aureus* and its virulence factors are different<sup>21</sup>.

In the extracellular environment, when facing opsonophagocytosis of the innate immune system, *S. aureus* has a polysaccharide microcapsule and protein A that binds to the Fc portion of immunoglobulin. This interaction inhibits opsonization ensuring no phagocytosis<sup>22</sup>. Also, acting on the innate and adaptive immune system. *S. aureus* has proteins such as chemotaxis inhibitory protein of *S. aureus* (CHIPS), extracellular adhesion protein (Eap), which, respectively, block neutrophil receptors for chemoattractants and neutrophil binding to endothelial adhesion molecule ICAM-1, inhibiting the migration of neutrophils from blood vessels to the infected tissues<sup>10,17,22</sup>.

Additionally, *S. aureus* produces exotoxins that have cytolytic activity. These are used to cause the leakage of the cell's content and lysis of the target cells<sup>10</sup>. The main known exotoxins are  $\alpha$ -hemolysin, Panton-Valentine leukocidin (PVL),  $\gamma$ -hemolysin and leucocidin that are responsible for cytolysis of the eukaryotic membrane on monocytes leukocytes and erythrocytes<sup>10,15</sup>.

In addition to the virulence mechanisms that *S. aureus* possesses, this bacterium induces the expression of genes encoding ROS detoxifying proteins, as is the case with catalase (*katA*), superoxide dismutase (*sodA*, *sodM*), thioredoxin reductase (*trxB*), thioredoxin (*trxA*), alkyl hydroperoxide reductase (*ahpC*, *ahpF*) and glutathione peroxidase (gpxA); and RNS as flavohemoglobins<sup>23</sup>.

#### 1.2. Iron sulfur clusters

The iron-sulfur clusters were initially described as catalytic centers in electron-transfer enzymes participating in biological functions, such as photosynthesis and respiratory electron transport chains<sup>24</sup>. These centers have various redox states, +2 and +3, achieving therefore, a high redox potential between -650 mV and +450 mV<sup>24–26</sup> because both iron and sulfur atoms have the ability to delocalize electrons by either donating or accepting multiple electrons<sup>27</sup>. This characteristic makes them ideally suitable for biological electron transport <sup>27</sup> particularly electron-transfer pathways between the surface and the active site of the protein.

Iron sulfur clusters are at the core of some proteins and these proteins are present in all kinds of organisms, including Archaea, bacteria, plants, and animals with high levels of evolutionary conservation. Fe-S clusters have been incorporated in metabolic pathways, such as photosynthesis thus contributing to the success of early life forms<sup>27</sup>. For example, multiprotein system proteins, such as Complex I (NADH: ubiquinone oxidoreductase) of the respiratory chain, contains seven Fe-S clusters that can provide electron-transfer at longer distances because of the increasing reduction potentials between each successive cluster in chain <sup>24,27</sup>.

Proteins bound to iron-sulfur ([Fe-S]) clusters, found in metalloproteins, have polynuclear combinations of iron and sulfur atoms<sup>26</sup>. The most common clusters are [2Fe-2S], [3Fe-4S] and [4Fe-4S] (Figure 1.1) with cysteines generally completing tetrahedral S coordination at each Fe site<sup>24,27</sup>. Of the existing cluster types, [2Fe-2S] and [3Fe-4S] proteins represent approximately 10% and the [4Fe-4S] proteins 90%<sup>27</sup>.

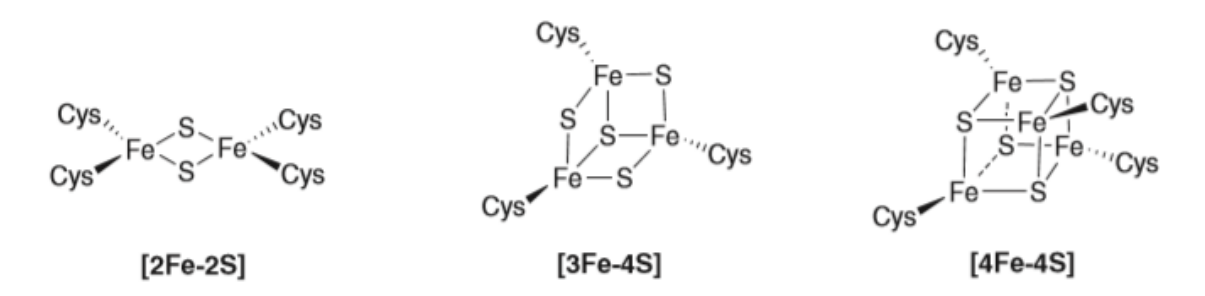


Figure 1.1 - The different types of [2Fe-2S], [3Fe-4S] and [4Fe-4S] and the corresponding structure.

Additional, Fe-S clusters are gene regulaters<sup>6,28,29</sup>, as clusters sense changes in iron, oxygen superoxide and nitric oxide. Under oxidative stress or iron deprivation conditions, the core of iron-sulfur proteins is oxidized therefore leading to protein function loss. In response to these

environmental stimuli, the transcription of numerous enzymes involved in cluster assembly mechanism, conversion, or redox chemistry is activated <sup>6,28,29</sup>.

In bacteria, there are three Fe-S cluster biosynthesis machineries, the lsc (iron sulfur cluster) system, the Suf (sulfur formation) system, and the Nif (nitrogen fixation). Even though these systems represent different pathways of Fe-S assembling, they perform similar functions<sup>30,31</sup>.

In *S. aureus*, the assembling of Fe-S cores and transfer of the Fe-S cluster to the target apoproteins is done by SufS, SufBCD, SufU, SufT, SufA, and Nfu. SufS is a cysteine desulfurase which catalyzes and transfers a sulfur atom to SufU, and this sulfur transfer protein transfers the persulfide to SufBCD machinery, which synthesizes [Fe2-S2] or [Fe4-S4] clusters. In this molecular scaffold, SufC is an ATPase, SufD has a role of acquiring iron and SufB is probably the scaffold protein, which is the site were the synthesis of the iron cluster occurs. After synthetizing the Fe-S core, it is transferred, through Nfu or SufA, to either an apoprotein or an Fe-S carrier, where SufS is an auxiliary factor maturation<sup>30,31</sup>.

## 1.3. Repair Iron Centers Protein

Repair of Iron Centers (RIC) protein, encoded in many bacteria, have the capability to restore the activity of oxidatively and nitrosatively damaged Fe-S enzymes<sup>6,29,32</sup>. In a large phylogenetic scale, the *ric* gene is present in bacterial species such as *Escherichia coli*, *S. aureus*, *Haemophilus influenzae*, *Salmonella spp.*<sup>28</sup>, among others and also in some eukaryotes such as *Trichomonas Vaginalis*<sup>5</sup>.

RIC protein is a non heme di-iron center<sup>7,33</sup> protein that is involved in the process of repair and restoring of the iron-sulfur clusters of metalloproteins in stress conditions, such as fumarase and aconitase enzymes, essential for cell survival, that are present in redox reactions of the cell's metabolism, more specifically in the tricarboxylic acid (TCA) cycle<sup>6,29</sup>.

When the bacteria are exposed to oxidative or nitrosative stress, the *ric* gene is expressed to protect Fe-S containing proteins and or enzymes to maintain their activity. Also it restores the activity of these damaged Fe-S clusters molecules<sup>7,34</sup> by giving iron to the scaffold protein iron sulfur cluster to IscU<sup>5</sup> along with IscS, that participate in the biosynthesis of iron sulfur cluster proteins.

Also, RIC is essential for *S. aureus* survival in activated macrophages and in the infection model *Galleria mellonella* it was shown that larvae infected with *S. aureus* wild type have a lower survival rate compared to  $\Delta ric$ . mutant. Therefore, RIC contributes for *S. aureus* pathogenesis to acquire full virulence in the process of infection<sup>34</sup>.

Additionally, in *E. coli* RIC also interacts with other proteins, such as Dps (DNA-binding protein from starved cells) in the detoxification and protective mechanism of ROS. Dps, belongs to the ferritin superfamily and it has a biochemical dual function for iron storage/iron oxidation modulation and DNA protection from oxidative stress<sup>35</sup>. The interaction between Dps and RIC are crucial to protect *E. coli* from ROS because the cells are sensitive to oxidative stress when the bacteria lacks one of the proteins<sup>32</sup>.

Furthermore, even in nonstress conditions, RIC restores the activity of enzymes such as aconitase and fumarase, meaning that RIC has a crucial role in maintaining, restore and protect the organisms' iron sulfur proteins<sup>34</sup>.

Structurally, RIC protein contains di-iron centers with a histidine/ carboxylate type within a four-helix bundle fold as illustrated in figure 1.2.

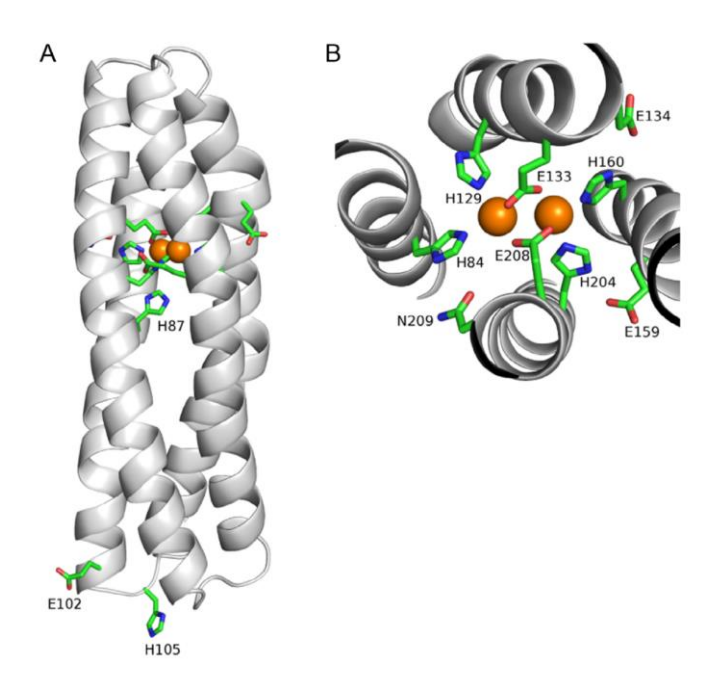


**Figure 1.2 -** Homology-based modelling of the *E. coli* RIC structure. In A the homology-based modelling is represented and in B a closeup view is show of the di-iron center. The di-iron center is coordinated by H84, H129, H160, H204, E133 and E20. The four-helix bundle (secondary structure) of the RIC protein is represented in gray. Adapted from reference<sup>36</sup>.

The di-iron present in this active center is coordinated by residues H84, H129, H160, H204, E133 and E208, where the E133 and E208 residues form two  $\mu$ -carboxylate bridges, which contribute

to the stability and functionality of the di-iron center<sup>7,33</sup>. Upon replacement of H129, E133, or E208 residues in *E. coli* RIC, the protein loses its ability to protect the aconitase activity. Also, the Apo-RIC is unable to recover damaged [Fe–S] proteins in vitro, suggesting that the non-heme carboxylate-bridged di-iron center is crucial for the RIC activity<sup>33</sup>.

RIC from *E. coli*, in its oxidized form, exhibits a UV-visible broad band at ca. 350 nm. As isolated, the di-iron is a  $\mu$ -oxo bridged mixed-valence Fe (II)/ Fe (III) binuclear center<sup>36</sup>, 56% in the oxodiferric form, corresponding to 78% and 22% of ferric and ferrous iron, respectively<sup>36</sup>.

Regarding the di iron release from the *E. coli* RIC protein to the reassembling system of iron sulfur cluster proteins, Fe (II) is more labile ( $K_{dRIC}$  10<sup>-13</sup> M) than Fe(III) ( $K_{dRIC}$  10<sup>-27</sup> M)<sup>33</sup>.

Throughout this thesis the study of the RIC protein of *S. aureus* JE2, which is a MRSA class strain that has a long predominance in the United States of America, was developed.

In *S. aureus* the RIC protein, also initially named ScdA<sup>23,28</sup>, has been identified as having a biochemical role very similar to *E. coli* YtfE in restoring the enzymatic activity of proteins such as aconitase and fumarase, when *S. aureus* cells are submitted to either nitrosative or oxidative stress inside macrophages, the  $\Delta ric$  mutant a has lower viability when exposed to oxidative stress, thus indicating a greater efficiency in protecting against oxidative than nitrosative stress. Structurally, these two proteins share 25% of identity and 46% of similarity to each other. They also present a high degree of conservation of the residues, mostly at amino acids that constitute the active center of the di-iron, namely, the residues His84, His105, His129, Glu133, His160 and His204 (numbering according *E. coli* YtfE)<sup>28</sup>.

Although these proteins are similar, and since the *S. aureus* RIC protein has a major role in oxidative stress, in order to characterize of *S. aureus* RIC protein functionality enzymatic, viability, oxidative stress resistance, complementation and protein-protein interaction assays were performed.

### 2. Aims and motivations

When humans are infected, the innate immune system is activated which will trigger the production and chemotaxis of phagocytes to the infection site to try to eliminate the threat. These phagocytes are neutrophils and macrophages that phagocytize bacteria and produce reactive nitrogen species (RNS) and reactive oxygen species (ROS) in order to cause cell damage in membranes and proteins essential for the pathogen cell metabolism.

However, bacteria have mechanisms to repair and minimize the damage caused by the immune system in order to maintain cell integrity. The main aim in this work is to study the RIC protein which is a non-heme di-iron center protein. This protein participates in the biosynthesis of sulfur iron centers in organisms such as *E. coli* and *S. aureus* and confers resistance to oxidative and nitrosative stress imposed by the innate human immune system. Specifically, our objectives throughout this dissertation were to;

- Test the viability and resistance of *S. aureus* and *E. coli* cells and their  $\Delta ric$  mutants when exposed to oxidative stress
- Determine if RIC has other functions in the cell, namely the catalase function, for this purpose, it is intended to carry out tests on the activity of cell extracts and with purified RIC protein.
- Investigate the role of residues that coordinate the di-iron center, by constructing site specific mutants of RIC from *Staphylococcus aureus*

## 3. Material and Methods

In this thesis the methicillin-resistant *S. aureus* (MRSA) strain JE2 was studied, that belongs to community-associated methicillin-resistant *S. aureus* strain USA300 LAC, *E. coli* K12ATCC and *E. coli* BW25113 (Table 3.1). All *S. aureus* strains grown overnight were grown in Tryptic Soy Broth (TSB) (BD Difco), at 37 °C, 150 rpm. The *E. coli* overnight growth was made in Luria-Bertani (LB) (Roth) at 37 °C, 150 rpm.

Table 3.1 - List of the bacteria and the different strains used.

Bacterium	Strain	Reference	
S. aureus	JE2	USA300 LAC <sup>37</sup>	
	JE2∆ <i>ric</i>	Nebraska Transposon Mutant	
		Library <sup>38</sup>	
	RN4220	Laboratory stock	
E. coli	K12ATCC	ATCC	
	K12Δ <i>ric</i> Justino <sup>39</sup>		
	BW25113 <i>katE</i>	Keio Collection	
	BW25113 katG	Keio Collection	
	BW25113 katEG	Laboratory stock	
	XL1	Agilent	
	BL21 DE3 Gold	Agilent	

## 3.1. Strain Complementation

### 3.1.1. DNA extraction

#### E. coli

The plasmid DNA in *E. coli* XL-1 was extracted using Mini Prep kit (Qiagen), according to the protocol After extraction of plasmid DNA, it was quantified in a Nanodrop ND-1000UV–visible spectrophotometer (Thermo Fisher Scientific) at 260 nm.

#### S. aureus

To extracted plasmid DNA in *S. aureus* RN4220, the same kit was used with a few alterations. To lys the cells, 80  $\mu$ g of lysostaphin were added, and the samples were incubated at 37  $^{\circ}$ C for 1 hour. After extraction of plasmid DNA, it was quantified in a Nanodrop at 260 nm.

## 3.1.2. Strain Transformation

#### S. aureus

The cells were thawed at RT for 10 min. Subsequently, they were centrifuged for one minute at 5000 rpm.

The supernatant was removed, and the cells were resuspended in 50  $\mu$ L of electroporation buffer (glycerol 15 % (Merck) and sucrose 0.5 M (Sigma)). To *S. aureus* RN4220 competent cells, 1  $\mu$ g of pDNA (table 3.2) was added, and the sample was transferred to an electroporation cuvette (BIO-RAD). A 2.5 V shock was applied for 2.5 ms. Immediately after electroporation, 900  $\mu$ L of 0.5 M TSB + sucrose medium was added. The cells were grown for 1 hour at 37 °C and 200rpm. 200 $\mu$ L of cells were plated into a TSA plate with the respective plasmid antibiotic, 10 $\mu$ g/mL chloramphenicol.

Electroporation was performed in JE2Δ*ric* competent cells with plasmids pMK4, pMK4-*ric*, pspac-pMK4-RIC, + pspac-pMK4-RIC-C30AC31A.

The same procedure was applied to the transformation of *S. aureus* JE2 cells except that 10 µg of pDNA was used.

**Table 3.2** - List of plasmids used for complementations. All of these plasmids were studied in *S. aureus*  $JE2\Delta ric$ .

Plasmid	Gene	Reference	
pMK4	-	Laboratory stock	
	+ RIC	Silva <sup>34</sup>	
pspac pMK4	+ RIC	This work	
	+ RIC C30AC31A	This work	

#### E. coli

Competent of katE, katG and katEG BW25113 cells were made. For this purpose, 3 pre inoculums were grown overnight with a different mutant at 37 °C and 150 rpm. The cells were cultured with 1% o/n growth in 20 mL of LB and the cells grew to an OD of 0.5. The sample was centrifuged for 5 min at 5000 rpm. Then, the supernatant was removed, and the pellet was resuspended in 4.5 mL of ice-cold 100 mM CaCl<sub>2</sub> and left in the ice for 1 hour. Afterwards, the samples were centrifuged again at 5000 rpm for 5 min and the pellet was resuspended in 600  $\mu$ L of 100 mM CaCl<sub>2</sub>. The cells rested for 1 hour on ice.

To each sample of competent BW25113 cells (table 3.3), 100 ng of each plasmid (pMK4, pMK4 + RIC, pUC18, pUC18 + RIC) were added and the cells rested on ice for 30 minutes. A thermal shock of 45 s at 42  $^{\circ}$ C was applied and the cells were immediately placed on ice. 900  $\mu$ L of LB was added and the cells were incubated at 37  $^{\circ}$ C and 180 rpm.

Cells were plated onto LB agar with the corresponding antibiotic, ampicillin 100 mg/mL to both pMK4 and pUC18 plasmids.

**Table 3.3 -** List of plasmids used in *E. coli* for complementation assays.

Strain	Plasmid	Gene	Reference
BW25133 katE	pMK4	+RIC	This work
	pMK4		Laboratory Stock
	pUC18	+ YftE	This work
	pUC18		Laboratory Stock
BW25133 katG	pMK4	+RIC	This work
	pMK4		This work
	pUC18	+YftE	This work
BW25133 katEG	pMK4	+RIC	This work
	pMK4		This work
	pUC18	+ YftE	Nobre 2015
XL1	pET24	+ RIC G128E	This work
	pET24	+ RIC G128E A169E	This work

## 3.2. DNA Cloning

A DNA fragment of 750 bp containing the *S. aureus ric* gene was PCR-amplified from pET24-RIC using the primers forward (5´-GGAGATATACATATGGCTAGCATGATAAAT-3´) and reverse (5´-CTTGTCGACGGAGCTCGGATCCTTTTTG-3´). The pspac-pMK4 vector and the *ric* gene were digested using the Nhel (NewEngland Biolabs) and BamHI-HF (NewEngland Biolabs) restriction enzymes. Afterwards, DNA ligase ligated the *ric* gene into the vector.

The plasmid was sequenced to confirm the absence of undesired mismatches After confirming the sequencing of the cloned gene, the resulting vector (pspacpMK4-RIC) was electroporated (1 µg) into *S. aureus* RN4220 and transformed cells were selected on TSA medium containing 10 µgmL<sup>-1</sup> chloramphenicol.

The recombinant plasmid extracted from *S. aureus* RN4220 cells was electroporated (10  $\mu$ g) into *S. aureus* JE2 $\Delta$ *ric*.To verify the transformed cells a PCR pDNA was made. The *ric* gene was amplified using the primers M13 forward (5´-GTAAAACGACGCCAG-3´) and reverse (5´-CAGGAAACAGCTATGAC -3´) To observe the amplified product, the samples were loaded with 1  $\mu$ L of loading buffer 5x into an agarose gel 1%. Electrophoresis was performed for 25 minutes at 80 V, 400 mA.

The same procedure was done to the mutant RIC-C30AC31A.

### 3.3. Protein purification

#### 3.3.1. Protein Expression

The *ric* gene expression was made in *E. coli* BL21 cells, in minimal medium M9 salts (0.2 mM MgSO<sub>4</sub>, 0.1 mM FeSO<sub>4</sub>, 0.1mM CaCl<sub>2</sub>, 20 mM Glucose) as described<sup>29</sup> in 1.5 L 3L Erlenmeyer at 180 rpm 30 °C until growth reached OD<sub>600 nm</sub> = 0.3 to be induced with 0.2 mM IPTG (thiogalactopyranoside) (Apollo Scientific) freshly made. After the induction, cells grow for 7 hours at 120 rpm and 30 °C, the cells were then collected by centrifugation at 8000 rpm at 4°C and frozen at -20°C.

#### 3.3.2. Protein Purification

Cells obtained were resuspended in buffer (20 mM Tris + 10% glycerol pH 6.96). These cells were lysed at 1000 psi in the French press (Thermo Fisher). The separation of the lysed cells from non-broken cells was made by centrifugation (8000 rpm, 4 °C, 30 min). The pellet (unbroken cells)

was separated from the supernatant (broken cells). The separation of the membrane fraction from the soluble fraction of the supernatant through an ultracentrifugation (42000 rpm, 4°C, 1: 30h) was made.

The supernatant was dialyzed in buffer (20 mM Tris + 10% glycerol pH 6.96) on a 12/14 kDa membrane (Roth) overnight with constant stirring at 4 °C.

Before proceeding to the chromatography, the sample was centrifuged at 13000 rpm for 15 minutes. The sample was injected into an AKTA Prime Plus (GE Healthcare) with an exchange chromatography column Q-sepharose 60 ml fast flow (GE Healthcare), pre-equilibrated with buffer (20 mM Tris + 10% glycerol pH 6.96). The column was washed with 1 column volume of buffer in order to remove the protein that did not bind to the column, then the sample that interacted with the column was eluted with a gradual gradient up to 20%, 40%, 60% up to 100% of elution buffer (20 mM Tris + 10% glycerol pH 6.96), in which 2 column volumes of buffer were passed in each gradient step. All injection and elution processes were monitored at 280nm.

Protein purity was evaluated by sodium dodecyl sulphate – polyacrylamide gel electrophoresis (SDS-PAGE) using a Mini-PROTEAN® Electrophoresis System (BIO-RAD). Samples, containing RIC protein were heated at 100  $^{\circ}$ C for 5 minutes and then the samples were loaded with 5  $\mu$ L of loading buffer (Tris-HCl 50 mM, pH8; SDS; Bromophenol Blue; Glycerol;  $\beta$ -mercaptoethanol) into the SDS-PAGE gel for 70 minutes to 150 V, 400 mA, 200 W in 4 % and 12.5 % acrylamide stacking and resolving gel respectively. Low molecular weight (LMW) standards (GE Healthcare) were used ranging from 14 to 97 kDa. Protein bands were revealed using Blue Coomassie Stainer (0.1 %).

Most pure fractions eluted in the ion Exchange chromatography were injected again in the AKTA Prime Plus equipped with a size exclusion Superdex 75. RIC was eluted with 20 mM tris + 10 % glycerol + 150 mM NaCl pH 6.96 buffer.

Evaluation of the fraction's purity was done through SDS-PAGE.

## 3.4. Oxidative stress assays

In the oxidative stress tests, two JE2 and JE2 $\Delta ric$  cell growths were made. Cells were inoculated into 20 mL of LB were inoculated at OD<sub>600nm</sub>=0.1. The antibiotic erythromycin (10  $\mu$ g/mL) was added to the JE2 $\Delta ric$  because of the antibiotic resistance gene of the mutant.

After one hour, one of each inoculum sample was exposed to 20 mM hydrogen peroxide  $(H_2O_2)$  (Sigma). The growth proceeded at 150 rpm at 37 °C for 8 hours, measuring points at OD  $_{600nm}$  every hour. Controls were performed without exposing the cells to  $H_2O_2$ .

## 3.5. Viability assays

In viability assays, the Colony Formation Units (CFU) is used to count any number of bacteria using dilutions, excluding dead bacteria and debris<sup>40</sup>.

From the *S. aureus* growing cultures used in the oxidative stress,  $100 \, \mu L$  of each growth was pipeted into a 96-well plate, where successive dilutions were made in phosphate-buffered saline (PBS) down the  $10^{-9}$  dilution. This test was carried out at the time of induction with oxidative stress and in the following 4 hours.

To proceed to the CFUs, 5  $\mu$ L of each dilution was pipeted into a Tryptic Soy Agar (TSA) (BD Difco) plate. The plates were incubated at 37  $^{\circ}$ C for 15 hours.

## 3.6. Enzymatic assays

In any chemical reaction, the reagents and products are separated by an activation energy. The activation energy is the free energy difference of the reagents up to the transition state. In the case of enzymatic catalysis, the activation energy decreases, so that the reaction occurs faster<sup>41</sup>.

Enzymatic kinetics allows the study of enzymatic catalysis, in which reaction rates are determined by varying numerous conditions, such as the concentration of the substrate, pH, temperature, among others<sup>41</sup>.

Experimentally, reaction rates are obtained by measuring either the appearance of the product, or the disappearance of the substrate. For this, it is necessary to guarantee the initial rate condition and the steady state hypothesis. The initial rate condition ensures that speeds can be determined from the tangent of the product concentration curve as a function of time<sup>42</sup>.

In the steady-state hypothesis, the substrate concentration must be a thousand times higher than the enzyme concentration in order to ensure that the concentration of the substrate enzyme complex is constant over time. By ensuring these conditions, the experimental reaction rates are measured (activity assays)<sup>42</sup>.

The activity assays are biochemical models to enzymatic studies. Even though this approach does not fully represent all enzyme mechanistic behaviors, it's a simple way to compare enzymatic systems.

#### 3.6.1. Catalase activity assays

#### S. aureus

To do the enzymatic activities assays, the *S. aureus* JE2 cells were grown in a 50 mL TSB medium at 37 °C with an agitation of 150 rpm. To follow bacterial growth, the optical density was measured at 600nm (OD 600nm) every hour. The cells were harvest at OD 0.6, 3 and 8 by centrifugation at 8000rpm for 15 minutes.

When mentioned, the cells were induced at OD 0.1 with 0.8 mM IPTG (isopropyl- $\beta$ -D-thiogalactosidaese) (Roth).

The cells were washed with 50 mM potassium phosphate buffer pH=7 (Fluka) and were resuspended in 250  $\mu$ L of the same buffer. In order to lys the cells, 20  $\mu$ g of lysostaphin (Sigma) were added and the cells were incubated for 1 hour and 30 minutes at 37°C.

Afterwards, the lysate was incubated with 250  $\mu g$  of DNAse (Roche) on ice for 10 minutes and then centrifuged for 15 minutes at 13000 rpm, to remove cell debris.

The enzymatic activities were assayed in a Shimadzu UV-1700. The catalase activity was followed by the decomposition of  $H_2O_2$  at 240 nm in a reaction mix of 5  $\mu$ L of *S. aureus* extract and 50 mM potassium phosphate buffer pH=7, with constant agitation at RT. Different concentrations of  $H_2O_2$ , 5, 10 and 20 mM, were tested.

To *S. aureus* WT and  $\Delta ric$ , as well for the complemented strains: JE2 $\Delta ric$  + pMK4, JE2 $\Delta ric$  + pMK4-RIC, JE2 $\Delta ric$ +pspac-pMK4-RIC and JE2 $\Delta ric$  + pspacpMK4-RIC-C30AC31A, the same protocol was applied except in the growth where the respective resistance antibiotics were added to the cultures 10 µgmL<sup>-1</sup> of erythromycin (Roth), to JE2 $\Delta ric$  mutant were added and to the cells with plasmid 5 µgmL<sup>-1</sup> chloramphenicol (Roth) were added.

#### E. coli

The cells of *E. coli* K12 ATCC, K12Δ*ric*, BW25113 *katE*, BW25113 *katE*+pUC18, BW25113 *katE*+pUC18-YftE, BW25113 *katE*+pMK4, BW25113 *katE*+pMK4-RIC, BW25113 *katG*, BW25113 *katG*+pUC18, BW25113 *katG*+pWK4-RIC, BW25113 *katG*+pWK4-RIC, BW25113 *katEG*, BW25113 *katEG*+pUC18, BW25113 *katEG*+pUC18- YftE, BW25113 *katEG*+pUC18- YftE, BW25113 *katEG*+pMK4, BW25113 *katEG*+pMK4-RIC (table 1.3) cells were grown in a 50 mL LB medium, at 37 °C, shaking 150 rpm. To follow bacterial growth, the optical density was measured at 600 nm every hour. The cells were harvested at OD 0.6 by centrifugation at 8000 rpm for 10 minutes.

The cells were washed with 50 mM potassium phosphate buffer pH=7 and were resuspended in 250  $\mu$ L of the same buffer. In order to lys the cells, 500  $\mu$ g of lysozyme (Sigma) were added, and the cells were incubated for 10 minutes at 37  $^{\circ}$ C.

Afterwards, the lysate was incubated with 250 µg of DNAse on ice for 10 minutes and then centrifuge for 15 minutes at 13000 rpm, and then the extract was separated from the pellet.

The enzymatic activities were assayed in Shimadzu UV-1700. The catalase activity for *E. coli* K12 ATCC and K12 $\Delta$ *ric* cell extract was followed by decomposition of H<sub>2</sub>O<sub>2</sub> at 240 nm in reaction mix of 20  $\mu$ L of *E. coli* extract and 50 mM potassium phosphate buffer pH=7 with constant agitation at RT. Different concentrations of H<sub>2</sub>O<sub>2</sub>, 5, 10 and 20 mM, were tested.

For the *E. coli* BW25113 extract cells, the catalase activity was followed by decomposition of  $H_2O_2$  at 240 nm in reaction mix of 5  $\mu$ L of *E. coli* extract and 50 mM potassium phosphate buffer pH=7 with constant agitation at RT.

### **RIC** protein

The enzymatic activities of the RIC protein activity were followed by decomposition of 10mM  $H_2O_2$  10mM at 240 nm in a reaction mix of 0.19 ng of protein with 50 mM potassium phosphate buffer pH=7 with constant agitation at 37°C.

To calculate the RIC specific activity ( $\mu$ mol / (min mg<sub>protein</sub>)) H<sub>2</sub>O<sub>2</sub> was used extinction coefficient of 43.6 mM<sup>-1</sup> cm<sup>-1</sup> was used. Measured initial rate (V<sub>0</sub>) was plotted vs substrate concentration. The Michaelis-Menten equation was used to create fitting curves to the experimental data, using a non-linear least-squares regression analysis in Graph Pad to determine K<sub>M</sub> and V<sub>max</sub> values.

## 3.7. Protein quantification of cell extracts and purified protein

The bicinchoninic acid (BCA) method was used to quantify the total protein present in the extract and purified protein. For this purpose, the protein standard used for the calibration curve was bovine serum albumin protein (BSA) (Sigma) at concentrations between 0 and 2 mgmL-1. The extracts were diluted to a 20 fold.10  $\mu$ L of each sample was pipetted into wells of a 96-well plate and 200  $\mu$ L of the BCA reagent (reagent A and reagent B in the proportions of 80: 1) (Thermo Fisher Scientific) was added. The plate incubated for 30 minutes at 37 °C. The absorbances were measured in the reader at 562 nm.

#### 3.8. Iron Quantification

The TPTZ method allows the iron quantification of the proteins by precipitating the protein and then reducing the iron.

Initially, 25  $\mu$ L HCL 8M were added to 20  $\mu$ M of protein and vortexed. The sample was incubated for 10 minutes at room temperature. Then, 25  $\mu$ L of TCA 80% were added and the sample was centrifuged for 10 min at 12000 rpm, the supernatant, 200  $\mu$ L, was remove to a 96 wells plate, and afterwards, it was added 50  $\mu$ L of ammonium acetate 75% and 20  $\mu$ L of hydroxylamine 10% were added, followed by agitation. Furthermore, 20  $\mu$ L of TPTZ were added, the plate was agitated, and the samples were incubated for 10 minutes at RT. The absorbance of the samples was read at 593 nm in a Multiskan <sup>TM</sup> FC Microplate Photometer (Thermo Fisher). The same was made to the iron calibration curve.

## 3.9. Protein-protein interaction studies

Bimolecular fluorescence complementation (BiFC) assay is a method that allows to study the protein-protein interactions in vivo. This technique consists of using vectors, in this case, pET11a-link-N-GFP and pMRBAD-link-C-GFP that express the green fluorescent protein (GFP) to allow formation of corresponding N- or C-terminal GFP fusions, respectively, which, when interacting, emits fluorescence that can be observed in a microscope<sup>43</sup>.

In this assay, the gene containing ric and dps was PCR amplified from the genomic DNA of S. aureus using the following forward (5'-GAGGTTATCTACCATGGTAAATAAAAATGAC -3') (5'-ATACACTGGACTCGAGGAGGTTATC-3') (5'and reverse CTAATCGCGTTGACCTCGATACTTTTT -3') (5'- TGGACGGATCCTTGCCAACAGTTTC-3') forward (5'-GACGTAGACAATCTCGAGGAGTGTATT-3') (5'primers for ric and GTATTAACCATGGTAATCAACAAGATGT-3') (5'and CTTATCTGTAGACGTCCTTAAGTAAGATTT-3') (5'-GGCTTTTATGGATCCTATTACTTATCTG-3') for dps. The amplified product was cleaned using QIAquick PCR purification (Qiagen).

Afterwards, *ric* was digested at 37 °C for 1:30 hours using XhoI and BamHI (for cloning into pET11a::link-N-GFP) and the at NcoI and Aat II sites (for cloning into pMRBAD-link-C-GFP). The same procedure was done to *dps*, pET11a and pMRBAD.

The *ric* and *dps* genes were ligated to pET11a and pMRBAD using DNA ligase for 16 hours at 16° C in a bath.

The resulting plasmids were transformed into XL1 *E. coli* ultracompetent cells. The cloning of the recombinant plasmids was confirmed through sequencing.

Cells harboring pET11a-link-N-GFP and pMRBAD-link-C-GFP served as negative controls and cells harboring pET11a-dps-N-GFP and pMRBAD-yftE-C-GFP (genes from *E.coli*) served as positive control.

*E. coli* BL21(DE3) Gold (Agilent) was cotransformed with the resulting recombinant pET11a-link-N-GFP and pMRBAD-link-C-GFP vectors to have the RIC/Dps and Dps/RIC combinations plated on selective LB agar with Ampicillin 100 mg/mL and chloramphenicol 35 mg/mL.

Posteriorly, colonies were inoculated in LB medium, grown overnight at 37°C and 150 rpm, and plated onto inducing LB agar medium containing 20 µM IPTG and 0.2% of arabinose at 30 °C overnight followed by 2 days of incubation at room temperature. For the analysis of the fluorescence of the cells, the colonies grown in the plate were suspended in phosphate-buffered saline (PBS) and spread onto 1.7% agarose slides. Cells were examined for green fluorescence in a Leica DM6000 B upright microscope coupled to an AndoriXoncamera, using 1000x amplification and a fluorescein isothiocyanate (FITC) filter. The images were analyzed using the MetaMorph Microscopy Automation and Image Analysis Software.

# 3.10. Site-Directed Mutagenesis

In vitro mutagenesis allows the study of protein function and genetic regulation<sup>44,45</sup>. Protein function can be changed only by changing one or more residues<sup>45</sup>. The manipulation of these residues consists of the mutation of one or more base pairs through site-directed mutagenesis.

This method, site-directed mutagenesis, allows the mutation of specific nucleotides using single-stranded oligonucleotides. Due to its simplicity, it is possible to introduce mutations in the RIC protein<sup>35</sup>. This technique uses a short synthetic DNA primer containing the mutation of choice (base changes, deletions, or insertions), which is then hybridized to the template DNA containing parental gene of interest (GOI). Using the PCR technique, the hybridized primer is then extended using DNA polymerase to replicate the plasmid containing the GOI. Afterwards, the template DNA is degraded by enzymatic digestion with a restriction enzyme specific for the methylated template DNA in order to only have mutated plasmid to be inserted into host vector. The mutation of GOI is then confirmed through sequencing<sup>46</sup>.

Mutated proteins of *E. coli* RIC were constructed by site-directed mutagenesis using 40 ng of each plasmid, pet24-RIC and pet24-RIC–GxxxE (already constructed in the lab). The mutations were done using the QuikChange II Site-Directed Mutagenesis Kit (Agilent Technologies) along with the

designed primers reverse (5'- CTAACAATTCTCCCGTTTCAATGTGGTCTGAAAC-3') and forward (5'-GTTTCAGACCACATTGAAACGGGAGAATTGTTAG-3'). Using the manufactures protocol, *E. coli* XL10-Blue competent cells (Agilent Techonologies), were transformed using 20  $\mu$ L of each reaction mixture by thermal shock at 42 °C for 30 s.

The cells grew for one hour at 37 °C and 150 rpm in LB media. The positive recombinant vectors were selected on LA plates containing 30 µgml<sup>-1</sup> kanamycin.

### 4. Results and Discussion

To characterize *S. aureus* RIC protein functionality, specifically its detoxifying role inside the cell under oxidative stress conditions, several experiments were used, such as viability and resistance to oxidative stress assays, enzymatic activities of the RIC protein and cell extracts.

In addition to these assays, a protein-protein interaction of RIC-Dps within the cell was studied. Also, some RIC protein residues were mutated in order to understand how these residues may influence the functionality of the protein because of its high conservation in different species.

# 4.1. Oxidative stress resistance and viability assays

In the oxidative stress and viability assays, the main goal was to determine if RIC conferred resistance to JE2 cells under oxidative stress conditions. This allows to evaluate the contribution of this protein to the survival and detoxification capacity of *S. aureus* bacteria under oxidative stress. The cell viability and resistance to oxidative stress were tested by exposing JE2 and JE2 $\Delta$ *ric* cells to hydrogen peroxide.

In the oxidative stress experiments (figure 4.1), the JE2 e JE2 $\Delta$ ric cells were exposed to 20 mM of hydrogen peroxide after one hour of growth, approximately at OD<sub>600nm</sub> of 0.2 of growth, and cell growth was monitored for 7 hours after oxidizing agent exposure.

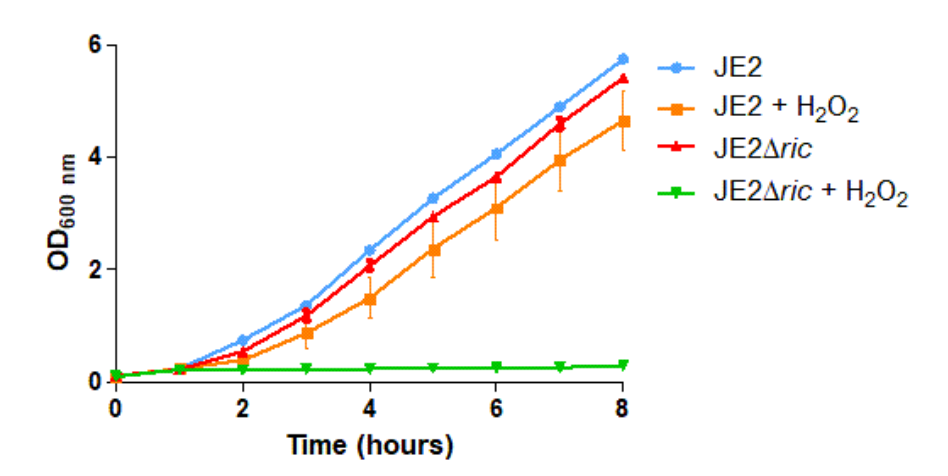


**Figure 4.1** - Representation of the growth curves JE2 and JE2 $\Delta$ *ric* strains in the oxidative stress assay. The samples JE2 (blue), JE2 $\Delta$ *ric* (red), JE2 + H<sub>2</sub>O<sub>2</sub> (orange) and JE2 $\Delta$ *ric* + H<sub>2</sub>O<sub>2</sub> (green) were grown for 8 hours and measurements were done hourly at OD at 600 nm. JE2 and JE2 $\Delta$ *ric* grew for 1 hour before being submitted to 20 mM of H<sub>2</sub>O<sub>2</sub>.

When the WT cells are exposed to 20 mM of  $H_2O_2$ , it is possible to observe a small decrease of the cell's growth, but they maintain the same profile as the JE2 control growth (figure 4.1. blue). This indicates that the wildtype has the ability to quickly restore the damage caused by ROS to maintain its proliferation. However, when the mutant is exposed to ROS (figure 4.1. green) the cells stop growing, thus indicating that RIC has a protective function to oxidative stress and that RIC is important for cell proliferation when cells are exposed to reactive oxygen species in the exponential phase of the growth.

Furthermore, cell viability was assessed as a complementary assay to the stress resistance experiment. This was done by testing cell viability (figure 4.2) before and 4 hours after adding  $H_2O_2$  20 mM to the JE2 and JE2 $\Delta$ *ric* cells growth (figure 4.1).

Initially, just before the cells were exposed to hydrogen peroxide (corresponding to 1 hour of growth), the CFU values were similar between the wild type and mutant (shown in white in figure 4.2).

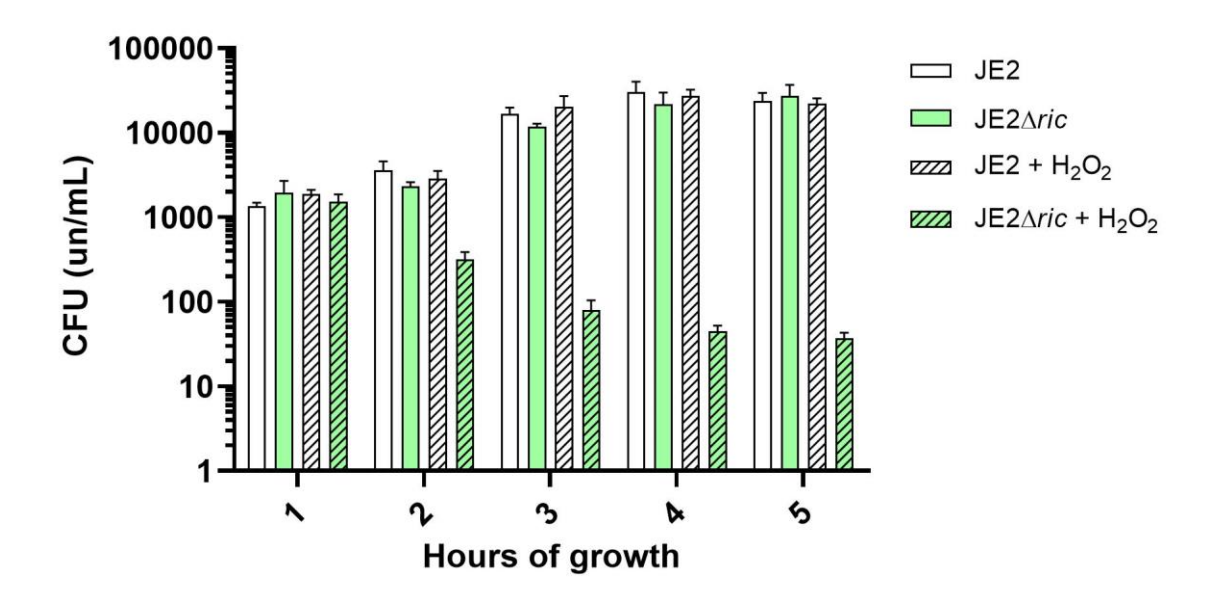


Figure 4.2 - Representation of JE2 e JE2 $\Delta$ *ric* cell viability. CFUs were obtained immediately before the addition of 20 mM H<sub>2</sub>O<sub>2</sub> and in the next 4 hours to test cell viability.

Overtime, after the JE2 and JE2 $\Delta$ *ric* cells were exposed to 20 mM of H<sub>2</sub>O<sub>2</sub>, it is observed a decrease in the viability of the JE2 $\Delta$ *ric* cells is observed, in comparison with the wt. This agrees with the growth curves shown above (figure 4.1) where the JE2 $\Delta$ *ric* strain stopped growing after hydrogen peroxide exposure.

In the case of viability tests, the JE2 cells, either exposed or not to hydrogen peroxide, maintained the same capacity to form colonies over time, thus demonstrating that the exposure to ROS only had a small influence on the JE2 cell viability.

Comparing the viability behavior of the JE2 WT with the mutant, when the JE2 $\Delta$ ric cells are exposed to hydrogen peroxide, its viability significantly decreases over time. Therefore, these data indicates that, when the mutant cells lacking the RIC protein are exposed to ROS, the cells stop proliferating and focus on detoxification and restoring processes to maintain cell viability. This, indicates that the RIC protein has an important role in the cell resistance to ROS.

## 4.2. Enzymatic activity assays

Afterwards, taking into account that RIC has been shown to protect, repair and restore against oxidative stress<sup>6,29,32,34,36</sup>, we wondered if RIC could have a catalase functionality. To complement the previous results, the determination of the enzymatic activity of RIC in the presence of H<sub>2</sub>O<sub>2</sub> was done. For this purpose, experiments were carried out by testing the enzymatic activity on purified *S. aureus* protein and on cell extracts of *S. aureus*, *E. coli* and their complemented strains.

#### 4.2.1. Catalase activity in cell extracts

For the study of the catalytic activity of RIC, extracts of JE2 and JE2 $\Delta$ ric were exposed to ROS. The cells were grown to an OD<sub>600nm</sub> of 0.6 (exponential phase), lysed and the cytoplasmic extract was collected to carry out the enzymatic assays. These extracts were exposed to 5, 10 and 20 mM hydrogen peroxide and the activity was determined in  $\mu$ mol / (min mg<sub>protein</sub>) for the different concentrations (figure 4.3).

By observing Figure 4.3, it is possible to see a difference in activity between the wild type and the mutant. At 5 mM, the wild type has an activity of 287  $\mu$ mol / (min mg<sub>protein</sub>) while the mutant has an activity of 80  $\mu$ mol / (min mg<sub>protein</sub>) which indicates that in the absence of RIC, there is a decrease of ~ 72% in activity.

The difference in the catalytic activity when exposing the wild type and the mutant to concentrations of 10 and 20 mM  $H_2O_2$  is also, approximately, 70%.

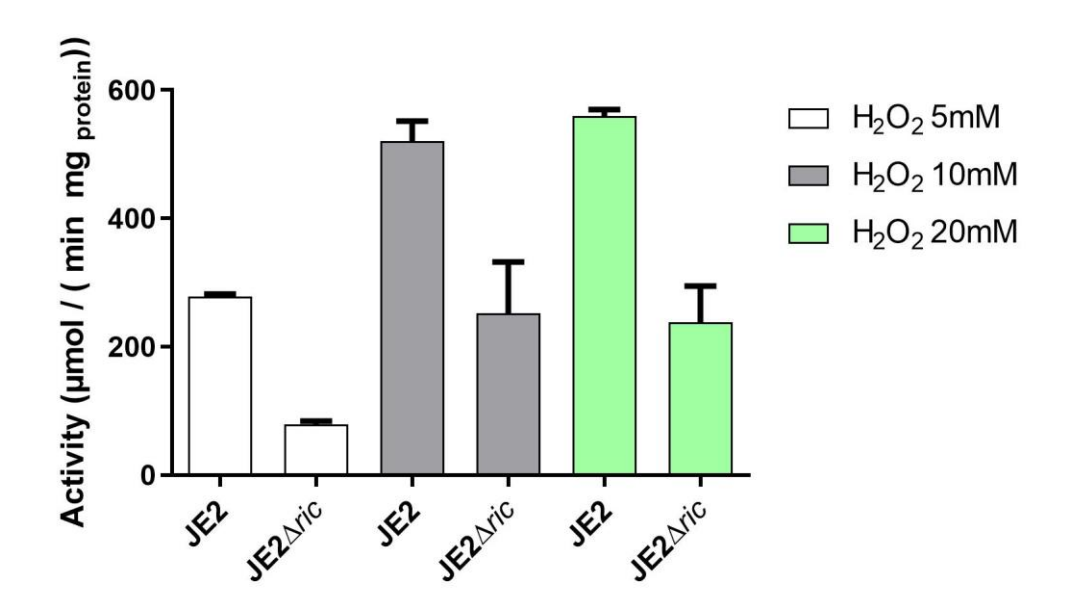


**Figure 4.3** - Representation of the enzymatic activity of JE2 e JE2 $\Delta$ *ric* extracts. The catalytic activity of JE2 e JE2 $\Delta$ *ric* extracts, grown in TSB to an OD <sub>600 nm</sub> of 0.6, was determine using 5 mM (white), 10 mM (grey) and 20 mM (green) de H<sub>2</sub>O<sub>2</sub>.

The catalytic activity of the wild type JE2 and the mutant JE2 $\Delta$ ric cytoplasmic extracts display a large difference in their maximum activity when exposed to hydrogen peroxide. Analyzing the activity of the extracts, it increases with increasing substrate concentration. However, comparing the wild type and the mutant activities, the difference between activities remains approximately 70%, which indicates that the RIC protein plays an essential role in protecting the bacteria in oxidative stress.

The RIC protein activity may be influenced by many factors, such as growth stages and nutrients and different growth conditions. Therefore, the activity of JE2 and JE2 $\Delta$ ric cell extracts was determined in different growth stages, optic density at 600 nm of 3 and 8, and in different media, LB or TSB medium. (Figure 4.4).

The results show a notable difference in the activity levels of cell extracts grown in LB vs TSB. Analyzing the catalytic activity of the samples grown in LB, the wild type activity, at  $OD_{600nm}=8$ , is 812 µmol / (min mg<sub>protein</sub>) comparing to the activity of 50 µmol / (min mg<sub>protein</sub>) forthe mutant. And at  $OD_{600nm}=3$ , the wild type activity is 636 µmol / (min mg<sub>protein</sub>), while the mutant has an activity of 186 µmol / (min mg<sub>protein</sub>).

In TSB the activity of the cell extracts is much lower in comparison with the activity obtained in LB grown cell extracts. As the wild type has a maximum activity of 231 and 197  $\mu$ mol / (min mg<sub>protein</sub>) and the mutant has an activity of 199 and 179  $\mu$ mol / (min mg<sub>protein</sub>) at OD<sub>600nm</sub>=8 and OD<sub>600nm</sub>=3,

respectively. Based on these activity values, there are no significant differences between the enzymatic activity of the wild type and the mutant cell extracts.

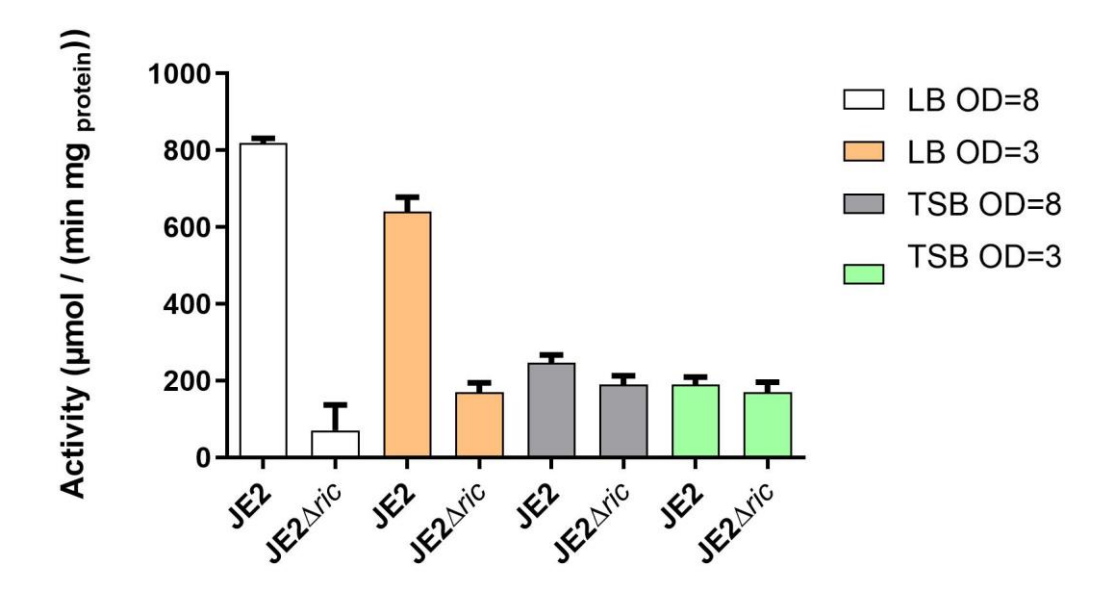


Figure 4.4 - Representation of the enzymatic activity of JE2 and JE2 $\Delta ric$  at different OD<sub>600nm</sub> and in different media, LB and TSB. All tests were performed with 10 Mm H<sub>2</sub>O<sub>2</sub>. JE2 and JE2 $\Delta ric$  cells were grown in LB up to OD<sub>600nm</sub> = 8 (white) and to OD<sub>600nm</sub> = 3 (orange) and in TSB up to OD<sub>600nm</sub> = 8 (grey) and to OD<sub>600nm</sub> = 3 (green).

In cells grown in LB medium, the activity difference between JE2 and JE2 $\Delta$ ric cell extracts is 94% and 70% at OD 8 and 3 respectively. On the other hand, the extracts obtained in the cells grown in TSB, the difference in activity between the mutant and the wild type is approximately 20% and 10% at OD<sub>600nm</sub> at 8 and 3. These results indicate that, in the stationary phase of growth, the activity of the mutant approaches the same catalytic activity of the wild type, as demonstrated previously<sup>47</sup>, where JE2 and JE2 $\Delta$ ric cell extracts, grown to an OD of 8, had identical activity to H<sub>2</sub>O<sub>2</sub> as substrate.

At this phase of the growth, OD 8 and 3, the cells grown in TSB have a difference in activity of 9 / 14% in contrast with to the difference of 60% that is obtained in the exponential growth phase (OD = 0.6). This may indicate that the RIC protein has a function more directed to the exponential growth phase rather than to the stationary phase, in which it can be speculated that RIC has a capacity to protect bacteria in the process of host infection and, its contribution to virulence as already demonstrated $^{34}$ .

Comparing the total activity of JE2 in the different media, the activity of JE2 grown in LB is much higher than the activity obtained in cells grown in TSB. Additionally, the *ric* mutant presents a lower activity in cells grown in LB than TSB. This difference in activities between the mutant and the

wild type is probably due to the production of toxic metabolites during growth that influences the catalytic activity of RIC while exposed to hydrogen peroxide.

To understand if other RIC proteins could have catalase activity, he enzymatic activity of E.  $coli\, K12ATCC$  and E.  $coli\, K12\Delta ric$  strains was also determined at different concentrations of hydrogen peroxide. These cells were harvested at an  $OD_{600nm}$  of 0.6, broken and cytoplasmic cell extracts were used to test the activities. At lower concentrations of peroxide, such as 5 mM, the extracts of both strains have a similar activity of 50  $\mu$ mol / (min mg<sub>protein</sub>). With the increase in the  $H_2O_2$  concentration, the difference in activities between the wild type and the mutant resembles the difference in activity shown in figure 4.5.

At 10 mM of  $H_2O_2$ , the activity of the wild type is 68  $\mu$ mol / (min mg<sub>protein</sub>) and the activity of the mutant is 50  $\mu$ mol / (min mg<sub>protein</sub>). Furthermore, the activity of the wild type increases to 98  $\mu$ mol / (min mg<sub>protein</sub>) at 20 mM of  $H_2O_2$  while the activity of the mutant remains at 50  $\mu$ mol / (min mg<sub>protein</sub>). These results show that the activity of the wild type increases with higher amounts of  $H_2O_2$  but the mutant has the same activity throughout the different concentrations.

Comparing the results of *E. coli* with the results obtained in *S. aureus*, the catalytic activity for each concentration of peroxide is much lower for *E. coli*, which is in agreement with the fact that *E. coli* has a detoxification mechanism weaker than *S. aureus*. It is also demonstrated that the difference in activities between wild type and the mutant in *S. aureus* only happens to *E. coli* at higher concentrations of  $H_2O_2$ . These results demonstrate, once more, the importance of the RIC protein for ROS protection.

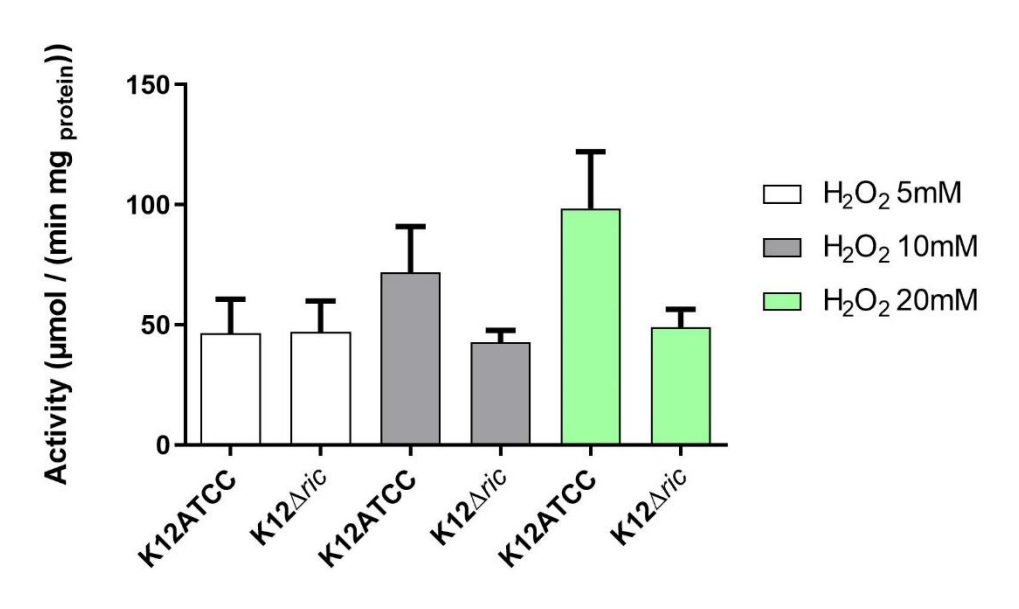


**Figure 4.5** - Enzymatic activity of *E. coli* K12ATCC and K12 $\Delta$ ric. The activity of the wildtype and mutant was determined using different concentrations of H<sub>2</sub>O<sub>2</sub> assays, 5mM (white), 10 mM de H<sub>2</sub>O<sub>2</sub> (grey) and 20 mM de H<sub>2</sub>O<sub>2</sub> (green).

#### 3.2.1.1. Complementation assays

In the complementation assays, it was intended to restore JE2 $\Delta ric$  mutant phenotype by complementing the mutant with a vector containing the *ric* gene to restore the cells extract activity in oxidative stress conditions<sup>48</sup>.

Initially, the plasmid containing the *ric* gene and an empty plasmid (serves as control to see if the plasmid influences the activity) were extracted from *E. coli* XL1 strains. Afterwards, the plasmids were electroporated into competent *S. aureus* RN4220 competent cells and the plasmid DNA was extracted again (to remove DNA methylations from *E. coli*). In order to confirm that the *ric* gene is present in the vectors, a colony PCR was performed, with the empty plasmid and the plasmid containing the *ric* gene.

JE2, JE2 $\Delta ric$ , JE2 $\Delta ric$  + pMK4 and JE2 $\Delta ric$ + pMK4-RIC cells were grown in TSB medium or LB medium up to an OD<sub>600nm</sub> of 0.6. The cells were then harvested and lysated. Enzymatic activities were performed with the cytoplasmic extract,.

As shown in figure 4.6 (A e B), the activity between the wild type and the mutant JE2 $\Delta ric$  shows a 50% difference in the total activity. Regarding the complemented strains, the activity of cell extracts with empty pMK4 is similar to the  $\Delta ric$  mutant, regardless of the medium and / or concentration of hydrogen peroxide.

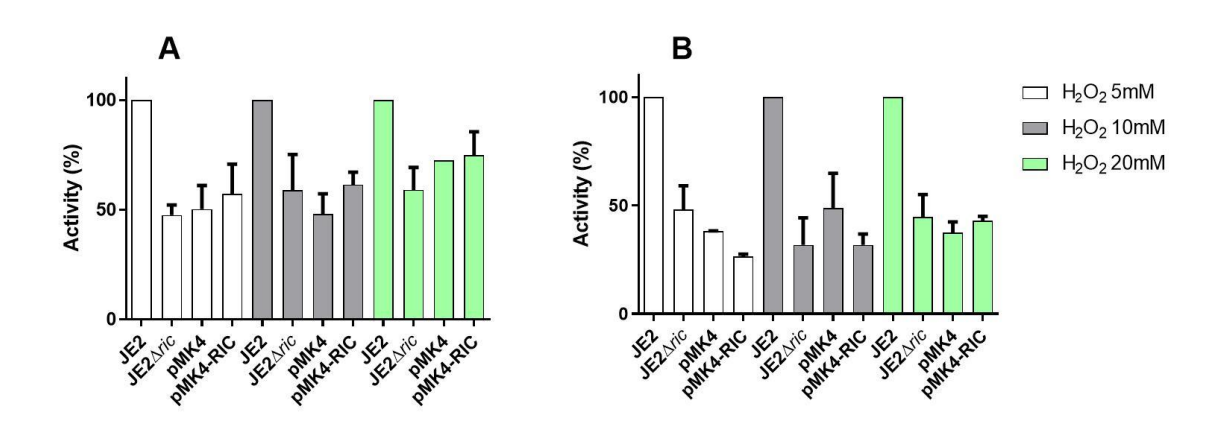


**Figure 4.6** - Representation of enzymatic activity in percentage of strains JE2, JE2 $\Delta$ *ric*, JE2 $\Delta$ *ric* pMK4 and JE2 $\Delta$ *ric* pMK4-RIC. Cell extracts grown in different media, TSB(A) and LB(B) to an OD of 0.6 and enzymatic activities were determine using three concentrations of H<sub>2</sub>O<sub>2</sub>, 5mM (white), 10mM H<sub>2</sub>O<sub>2</sub>, (grey) 20mM H<sub>2</sub>O<sub>2</sub> (green).

The difference in activity of WT to the mutants grown in TSB (figure 4.6 A) is smaller lower in comparison with extracts from cells grown in LB. This result could be due to TSB media being richer

in nutrients than LB, however the activity of the pMK4 + RIC mutant does not completely restore the activity to the wild type levels.

Concerning the vector containing the *ric* gene, the activity of the JE2 $\Delta$ *ric* pMK4-RIC cytoplasmic extract in LB (figure 4.6 B) is similar to the  $\Delta$ r*ic* mutant and the mutant with pMK4, which indicates that activity has not been restored.

Thus, these results indicate that the vector expressing RIC did not contribute to restore the WT strain phenotype.

Since the vector carrying the *ric* gene (being regulated by its own promotor) was not able to complement the mutant strain, an inducible IPTG promotor was used.

In these complementations, the inducible vector was constructed using *ric* or the RIC-C30AC31A mutated protein gene.

The RIC-C30AC31A lacks the cysteine residues that are highly conserved in RIC proteins<sup>33</sup> and are important for the RIC's oligomerization state<sup>49</sup>. Also, the Cys-Cys bridging bond mechanism may contribute to resistance of Mycobacterium proteins to the oxidative stress conditions within an infected host macrophage<sup>50</sup>. In this case, this mutant was used to understand if the structure of the RIC protein could affect the oxidation activity of  $H_2O_2$ .

The genes of RIC and RIC C30AC31A were amplified from plasmids previously existing in the lab and cloned into pspacMK4 to complement the JE2 $\Delta ric$ . *E. coli* XL1 cells were transformed with the plasmid of interest. To verify the transformed colonies, a colony PCR was made, followed by agarose gel electrophoresis. The plasmid was extracted from the *E. coli* cells and electroporated into *S. aureus* RN4220. Then, the plasmid was extracted from the *S. aureus* RN4220 and transformed into the *S. aureus* JE2 $\Delta ric$  strain.

The JE2, JE2 $\Delta$ ric, JE2 $\Delta$ ric+pspacpMK4-RIC and JE2 $\Delta$ ric+pspcapMK4-RIC C30AC31A were grown in different conditions, induced with 0.8 mM IPTG at the beginning of the growth or not induced, until the cells reached an OD<sub>600nm</sub> of 0.6. Then the cells were harvested, lysed, and the cytoplasmic extracts were isolated (figure 4.7).

In the non-induced samples, the difference in the enzymatic activity between the wild type (JE2) and the JE2 $\Delta$ *ric* mutant remains similar to the samples represented in figure 4.5. Regarding the complemented strains, it was observed that the JE2 $\Delta$ *ric*+pspacMK4-RIC and JE2 $\Delta$ *ric*+pspacMK4-RIC C30AC31A activity with 5 mM of hydrogen peroxide is higher than that of the JE2 $\Delta$ *ric* mutant. The samples were induced with 0.8 mM IPTG at the beginning of the growth.

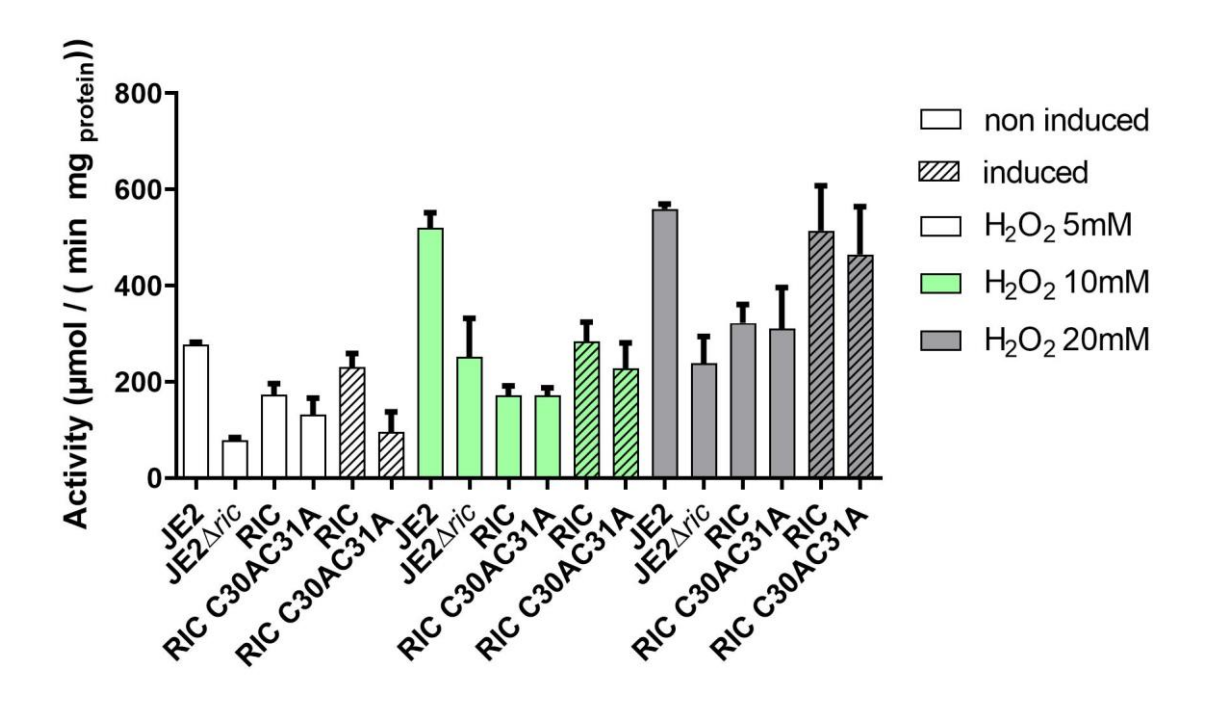


**Figure 4.7** - Determination of the enzymatic activity of *S. aureus* JE2, JE2 $\Delta$ *ric*, JE2 $\Delta$ *ric*+pspacpMK4-RIC and JE2 $\Delta$ *ric*+pspacpMK4-RIC C30AC31A extracts performed at 5 (white),10 (green) and 20 mM (grey) of H<sub>2</sub>O<sub>2</sub>. The cells grew to OD <sub>600nm</sub> = 0.6 in TSB. JE2 $\Delta$ *ric*+pspacpMK4-RIC and JE2 $\Delta$ *ric*+pspacpMK4- C30AC31A cells (stripes) were induced with 0.8 mM IPTG.

To test the RIC activity in a different phase of the cell growth, the cells were grown to an optical density at 600 nm of 3. Induced and non-induced conditions were tested to compare activities for the complemented strans, wild type and  $JE2\Delta ric$  mutant (figure 4.8).

As can be seen in figure 4.8, the enzymatic activity of the wild type at  $OD_{600nm} = 3$  is 236  $\mu$ mol / (min mg<sub>protein</sub>) which is similar to those obtained at OD 0.6 and 8 (figure 4.3 and 4.4).

The JE2 $\Delta ric$  mutant shows a decrease in catalase activity of about 40% compared to the wildtype as seen previously., When not induced, the mutant complemented with RIC and RIC-C30AC31A have an activity similar to the JE2 $\Delta ric$  mutant, On the other hand, when induced with 0.8mM IPTG, their activity increases to, 215 and 196  $\mu$ mol / (min mg<sub>protein</sub>) , respectively, similar to the wild type activity.

Initially, the complementation assays with plasmids pMK4 and pMK4-RIC were not successful since the activity of  $JE2\Delta ric$  +pMK4-RIC did not restore wild type's activity, regardless of the medium.

Subsequently, the *ric* gene was cloned into the inducible pspacMK4 vector, in order to complement the enzyme activity of the mutant. When induced the mutants  $JE2\Delta ric$ +pspacpMK4-RIC

and JE2 $\Delta ric$ +pspacpMK4-RIC C30AC31A, showed an activity similar to that of the wild type, thus indicating that the mutant restored activity in the presence of a vector containing the *ric* gene, demonstrating once again the importance of the RIC protein in protecting ROS.

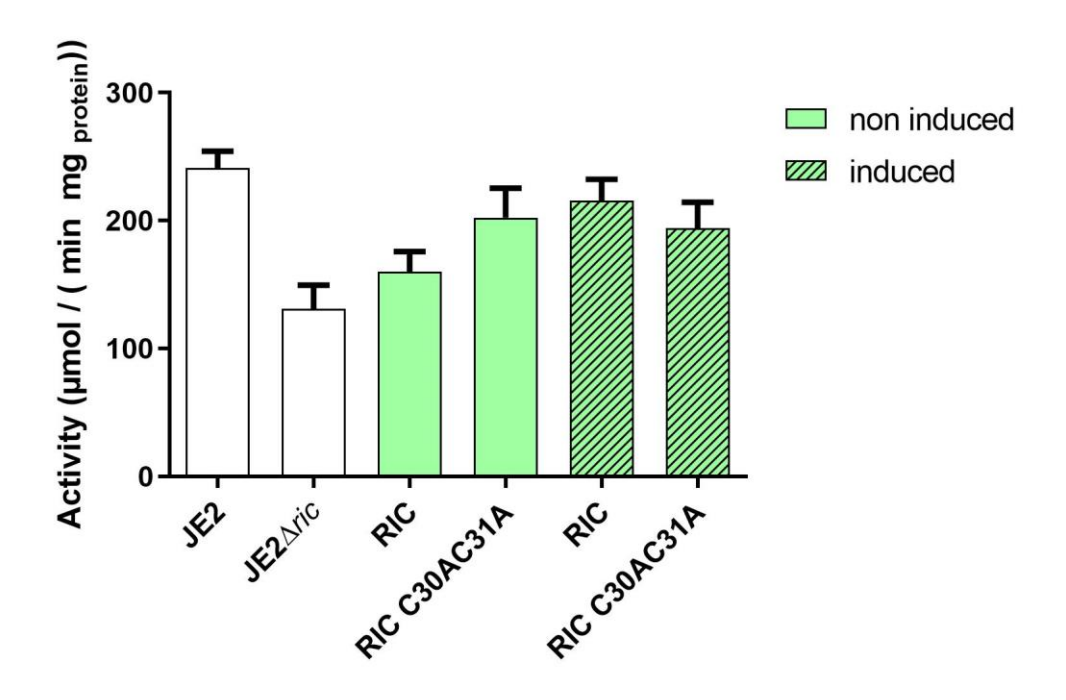


**Figure 4.8** - Enzymatic activity of the JE2, the mutant and the complemented strains extracts. All *S. aureus* cells grew until an OD of 3. JE2 $\Delta$ *ric*+pspacpMK4-RIC eJE2 $\Delta$ *ric*+pspacpMK4-RIC C30AC31A complemented growth (green) were non induced and induced with 0.8 of IPTG (stripes). All assays were performed with H<sub>2</sub>O<sub>2</sub> 10mM.

#### 4.2.2. Catalase activity with purified RIC protein

To determine the enzymatic activity of *S. aureus* RIC protein enzymatic activity, BL21 *E. coli* cells were grown in minimal medium in order to produce high-levels of GOI expression avoiding inclusion bodies.

The cells were grown, lysed and the cytoplasmic fraction was separated from the membrane fraction by centrifugation. To purify the protein, two types of chromatography were chosen, ion exchange and size exclusion chromatography. In ion exchange chromatography, several peaks were obtained in the elution of the different gradients.

The proteins of the cells lysed were injected into an HPLC system containing a Q-Sepharose Fast Flow ionic exchange column, in order to purify the RIC protein.

In the ionic exchange chromatography, several peaks were obtained in the elution of the non-linear gradient. The elution occurred with a gradient between 0 and 1 M NaCl (Figure 4.9).

Three peaks were obtained at a gradient of 20% NaCl, 1 peak at 40% NaCl, 1 peak at 60% eluent and a peak at 100 % NaCl.

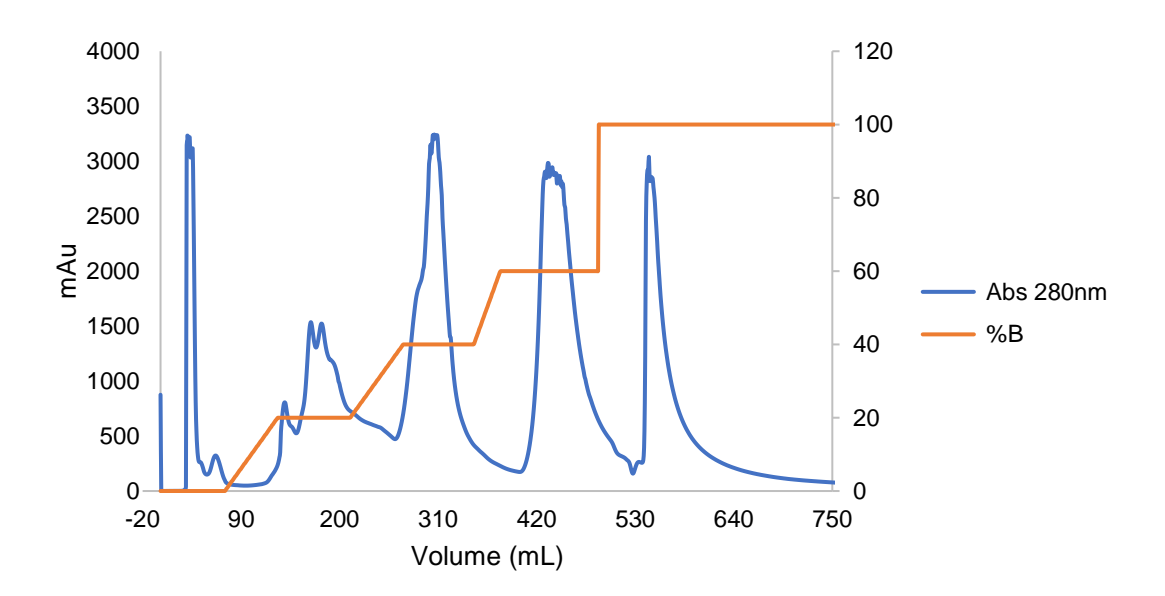


**Figure 4.9** - Chromatogram obtained in the purification of *S. aureus* RIC protein by a Q Sepharose-FF ionic exchange column. The absorbance at 280 nm (blue), represents the elution of samples at different ionic gradient (orange) of 1 M NaCl, 20 mM Tris + 10% glycerol pH 6.96 buffer. RIC protein was eluted at 40 % of elution buffer.

To identify the peak corresponding to the RIC, we proceeded with SDS-PAGE. The SDS-PAGE allowed to evaluate the efficiency with which the protein purification was performed.



Figure 4.10 - Image of size exclusion chromatography column purifying the RIC protein.

The purest fractions were then injected into the AKTA system for a size exclusion chromatography (Figure 4.10). In this chromatogram it is possible to observe that the proteins started to be eluted at 40 ml to 58 ml and that several peaks are present in a single peak (Figure 4.11).

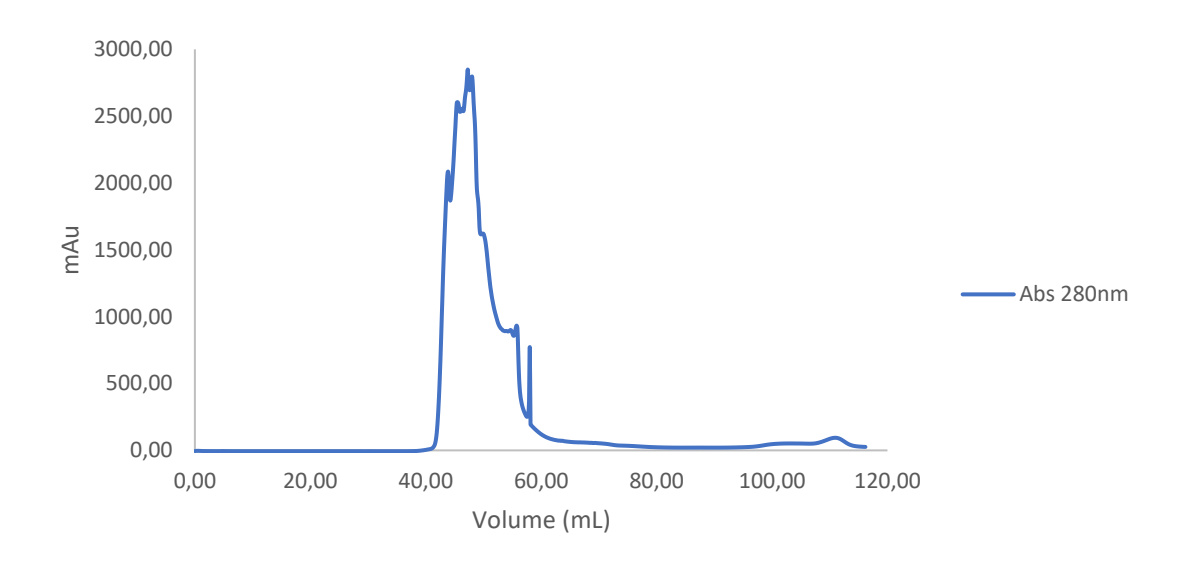


**Figure 4.11** - Chromatogram obtained in the purification of *S. aureus* RIC protein by size exclusion chromatography. The elution of the samples was followed at 280 nm (blue). RIC was eluted between 40 ml and 58 ml.

All fractions were analyzed trough a SDS-PAGE. The samples that have present less contaminants and have the band in the molecular weight corresponding to the RIC were mixed, concentrated and used for enzymatic activities (figure 4.12).

The protein concentration quantification was performed in two ways, using the BCA method and the UV-visible spectrum (Figure 4.13). In the BCA method, protein quantification was performed at the total protein quantity of the sample and obtaining the value of 10 mg mL<sup>-1</sup> was obtained.

In the spectrum, it is possible to observe a broad band at 350 nm characteristic of the RIC protein<sup>33</sup>.

Furthermore, the iron quantification assay determined that *S. aureus* RIC protein has two irons, like YtfE<sup>33</sup>.

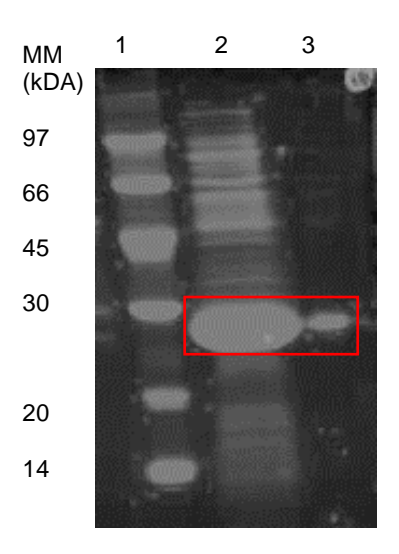


**Figure 4.12** - SDS-PAGE illustrating the RIC purification. SDS-PAGE: Stacking Gel – 4 % acrylamide; Resolving Gel – 12,5 % acrylamide; 1- Low molecular weight maker. 2 – Sample before purification. 3 -after purification. Molecular mass of RIC: 28 kDa.

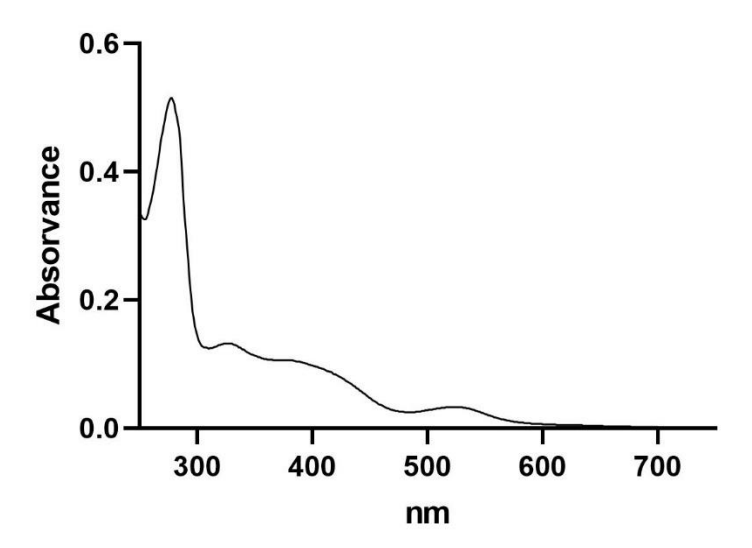
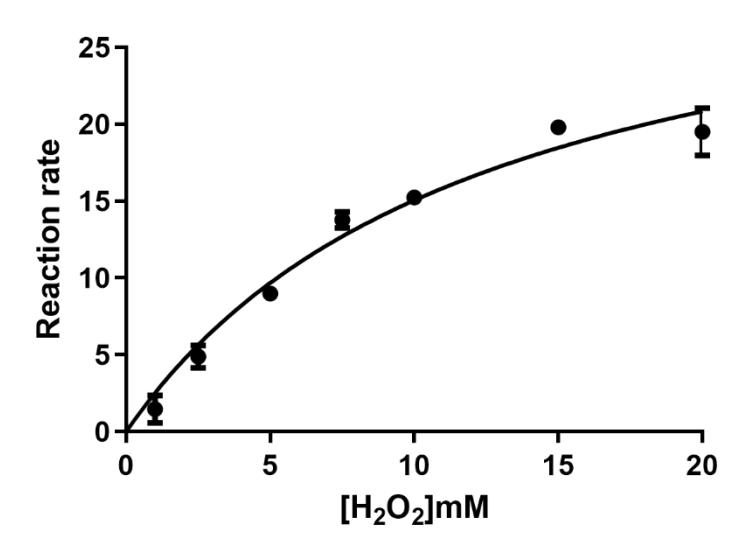


Figure 4.13 – UV-visible spectrum of the RIC protein.

The Repair Iron Center protein activity was measured from purified protein. The reaction was followed spectroscopically, at 240 nm, by measuring the substrate consumption  $(H_2O_2)$ . The the activity curve measured  $V_0$  was plotted vs the substrate concentration. The Michaelis-Menten kinetic model was used to obtain a fitting curve to the data (figure 4.14).

This model allowed to determine the kinetics constants  $V_m$  e  $K_m$ , 30.35 mmol / (min mg<sub>protein</sub>) and 15.94 mM, respectively.



**Figure 4.14** – S. aureus RIC protein kinetic curve of the reaction rate vs  $[H_2O_2]$  ranging from 0 to 20 mM. The curve in black line represents the fit obtained with the Michaelis-Menten equation. Specific activity was measured by following the decrease in absorbance at 240 nm ( $H_2O_2$  consumption) using 10 mM of S. aureus RIC protein.

Comparing these values with those of catalase present in the literature the KatA catalase of *Xanthomonas campestris pv. phaseoli*, a catalase similar to the *katA* catalase of *S. aureus*, has a Km value of 75mM<sup>51</sup>, thus being in the same order of magnitude as the result obtained for RIC which indicates that this protein may have a possible catalase role when bacteria are exposed to ROS.

## 4.3. Complementation of catalase mutants

After verifying the importance of the RIC protein in detoxification and or protection process of JE2 cells, we wanted to determine if the *S. aureus* RIC protein could complement the catalase activity in catalase mutants, even though the RIC protein has a low catalase enzymatic activity.

In order to test this hypothesis, the resistance to oxidative stress imposed on *E. coli* BW25113 cells and the respective mutants *katE*, *katG* and *katEG* began to be verified.

The *katE* and *katG* genes encode the bifunctional catalase-peroxidase (HPII) enzymes that are induced in the stationary phase and the monofunctional catalase (HPI) that is induced in the presence of oxidative stress, respectively. And these mutants were used in order to determine if RIC could also have a similar function to that of catalase<sup>52</sup>.

To determine the behavior of cells under stress conditions, an oxidative stress assay, similar to the one previously performed was done using *E. coli* BW25113 WT cells and *katE*, *katG* and *katEG* mutants. The cell growth was carried out for 6 hours and the cells were exposed to 5 mM  $H_2O_2$  after one hour of growth,  $OD_{600 \text{ nm}} \sim 0.3$  (figure 4.15).

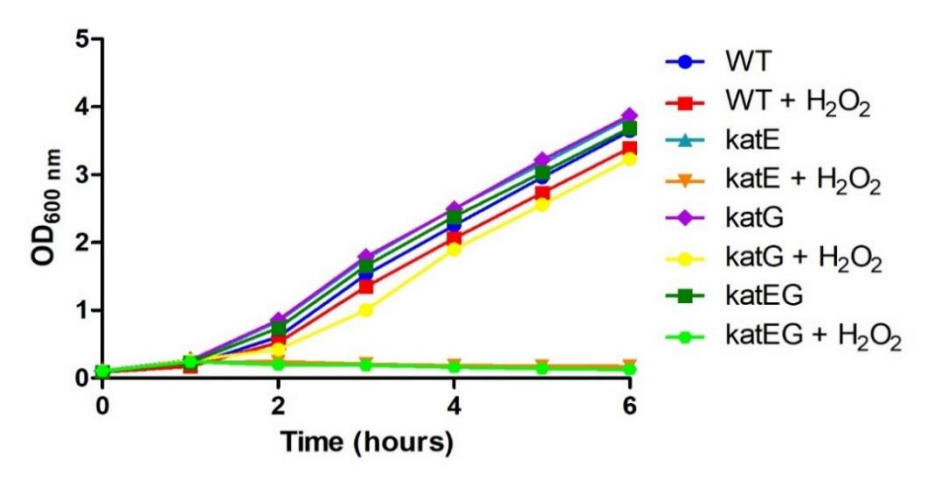


**Figure 4.15** - Representation of the growth curves of *E. coli* BW25113 WT and mutants *katE*, *katG*, *katEG* in the oxidative stress assay. The growth was monitorized by OD measurements at 600 nm hourly for 6 hours. The samples WT +  $H_2O_2$  (red) and  $katE + H_2O_2$  (orange),  $katG + H_2O_2$  (yellow),  $katEG + H_2O_2$  (green fluorescent) were exposed to 5 mM of  $H_2O_2$ . The WT, katE, katG, katEG controls are shown in blue, cyan, purple and dark green, respectively.

As shown in figure 4.15, it is possible to verify that the wild type (blue) and the mutants *katE* (cyan blue), *katG* (yellow) and *katEG* (dark green), corresponding to the control assays, have similar phenotypes under non-stress conditions.

However, in stress conditions, *katEG* and *katE* mutant cells stop growing, contrary to what happens with WT and *katG* which, despite their growth decreasing due to the exposure of the reactive oxygen species, continues to have the same behavior as the control growths.

The *katE* and *katEG* mutants lack the HPII protein. These genes are expressed essentially during the stationary phase and have a crucial role in cell survival Despite not being inducible peroxide<sup>53</sup> the results demonstrate that, these proteins are essential for bacterial survival under stress conditions.

Regarding these results, we intend to observe if, when these strains are complemented with *E. coli* or *S. aureus* RIC protein, if it was possible for the mutant to restore or protect iron sulfur clusters enzymes by having the RIC protein. All the mutant strains were complemented with the vectors pUC18 + YftE and pMK4 + RIC to check if the mutant strain phenotype can be reverted by the expression of RIC under oxidative stress during their growth (figure 4.16).

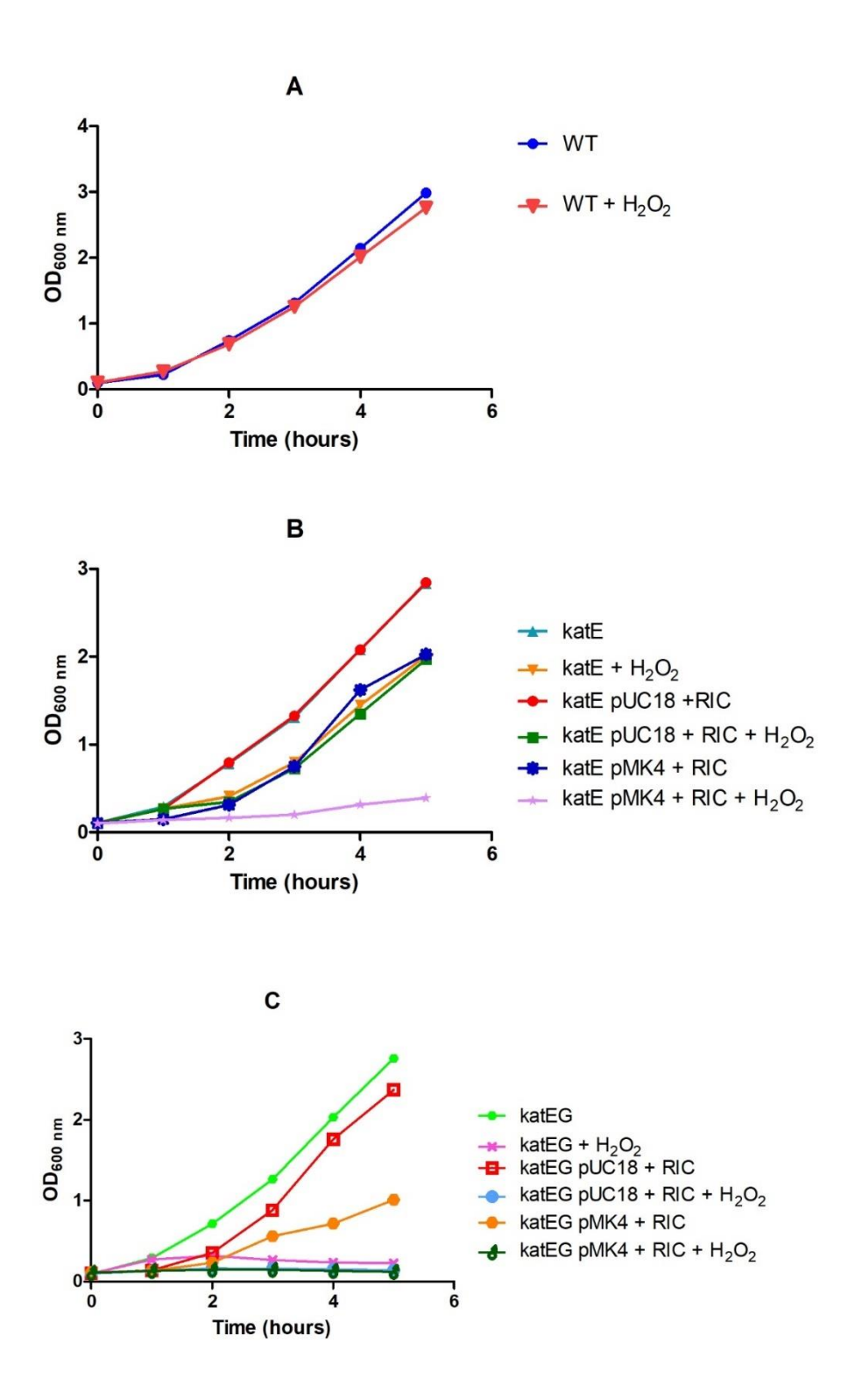


**Figure 4.16** - Oxidative stress assays of *E. coli* BW25113 WT and mutants *katE*, *katEG* and complemented strains (pMK4+RIC, pUC18+YtfE). The growth was monitorized by OD measurements OD at 600 nm hourly for 5 hours. The samples were exposed to 1 mM of H<sub>2</sub>O<sub>2</sub>. A- Representation of wild type growth (control, blue) and oxidative stress conditions (red). B – Growth curve of *katE*+pMK4+RIC, *katE*+ pUC18+ YtfE and *katE* mutants.

KatE +pMK4+RIC (dark blue), katE + pUC18+ YtfE (red) and katE (blue) mutants are represented as controls and katE +pMK4+RIC (pink), katE + pUC18+ YtfE (green) and katE (orange) as the growth exposed to ROS. C-Growth curve of katEG +pMK4+RIC, katEG + pUC18+ YtfE and katEG mutants. The control growth katE +pMK4+RIC (orange), katE + pUC18+YtfE (red) and katE (green) mutants and growth exposed to hydrogen peroxide katEG +pMK4+RIC (dark green), katEG + pUC18+ YtfE (blue) and katEG (pink) are represented.

After testing various concentrations of hydrogen peroxide, the concentration at which some difference in growth and phenotype was observed between the mutants and the complemented mutants was 1 mM  $H_2O_2$ .

Wild type exposure to peroxide did not have a major impact on growth. However, in the *katE* mutant (figure 4.16 B) a slight difference in growth is observed. *katE* and *katEG* pUC18 + YftE and pMK4 + RIC have impaired growth when the cells are exposed to ROS, thus RIC does not replace the catalase role in protecting *E. coli* of oxidative stress.

The growth curves of *katEG* mutant, in figure 4.16 C, show that all mutant cells stopped growing when exposed to oxidative stress.

As can be seen in the figure 4.16, the difference between WT and the mutants *katE* and *katEG* in growth when cells are exposed to 5 mM of hydrogen peroxide is identical to that presented in *S. aureus*. Therefore, when cells lack either Kat or RIC, growth is affected under oxidative conditions, thus leading to the possibility that RIC could have a catalase activity essential to protect and or detoxify the cells of oxidative stress.

Subsequently, when complementing these mutants, *katE* and *katEG* with pUC18 + YtfE or pMK4 + RIC plasmids, it was expected that the growth behavior, although a little inferior, to be similar to the controls (growths not exposed to peroxide). However, even though the cells were subjected to a lower concentration of ROS, 1 mM instead of 5 mM, the only mutant in which they complemented the phenotype was *kat E* pUC18 + YtfE, which indicates that RIC has a role in resistance as already described in the literature<sup>54</sup>.

In the complementation experiments on  $E.\ coli$  strains, the enzyme activity assays were performed with 5 mM H<sub>2</sub>O<sub>2</sub> with the strains BW25113 WT,  $katE,\ katG,\ katEG$  and complemented strains with pUC18 + YtfE or pMK4 + RIC plasmids (figure 4.16). Cells were cultured to an OD<sub>600 nm</sub> of 0.6. In general, the activity values of WT, complemented and non-complemented mutants are very similar to each other.

These results show that the non-complemented mutants, that do not have one or two (in the case of the *katEG* mutant) catalases that are present in the wild type, still displayed similar enzyme activity values. This may indicate that during this phase of the cell growth, the protein amount

expressed in *katE* and *katG* is not very significant. This result obtained for *katE* is contradictory to the statement in the literature in which *katE* plays a crucial role in the survival of the bacterial cell in the exponential phase<sup>52</sup>.

Regarding the enzymatic activity of each sample, regardless of the concentration of the substrate, the WT activity is similar to that of the *katE*, *katG*, *katEG* mutants and complementations (pMK4-RIC pUC18 - YtfE) (Figure 4.17).

Regarding the activity of the complemented strains, it is possible to verify that the complementation did not restore the WT phenotype.

Regarding the supplemented pMK4-RIC strains, since the complementation is done with the *S. aureus* RIC protein, it may have a modified function and or structure since it is expressed in an endogenous organism in order for the complementation not restoring the phenotype.

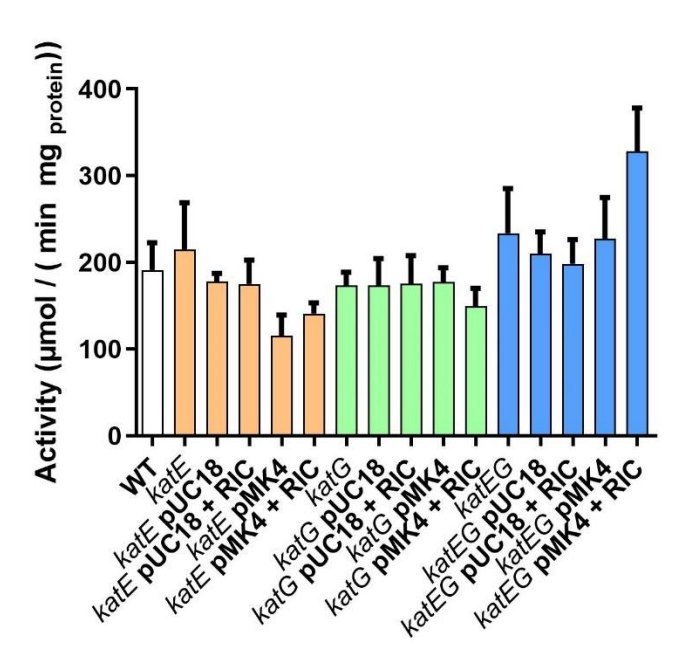


**Figure 4.17** - Determination of the enzymatic activity of *E. coli* BW25113 wild type (white), *katE* (orange), *katG* (green), *katEG* (blue) mutants and complementations (pMK4-RIC pUC18-YftE) extracts using 10mM of hydrogen peroxide. All cells were grown to OD 600nm = 0.6.

#### 4.4. Protein-Protein interactions

It was also analyzed whether the *S. aureus* RIC protein could interact with other proteins, namely *S. aureus* Dps, as previously described for the *E. coli* RIC in the literature<sup>32</sup>.

The interaction of these two proteins was done through a BiFC experiment. In this assay, when the two proteins interact, they emit fluorescence inside the cell.

Since this is comparative experiment, pET11a-link-N-GFP and pMRBAD-link-C-GFP empty plasmids were negative controls (C-) and cells harboring pET11a-dps-N-GFP and pMRBAD-yftE-C-GFP plasmids were the positive controls (C+). The fluorescence emitted from these controls was compared with the fluorescence emitted by the samples RIC<sup>N-GFP</sup> + DPS<sup>C-GFP</sup> and DPS<sup>N-GFP</sup> + RIC<sup>C-GFP</sup> (figure 4.18).

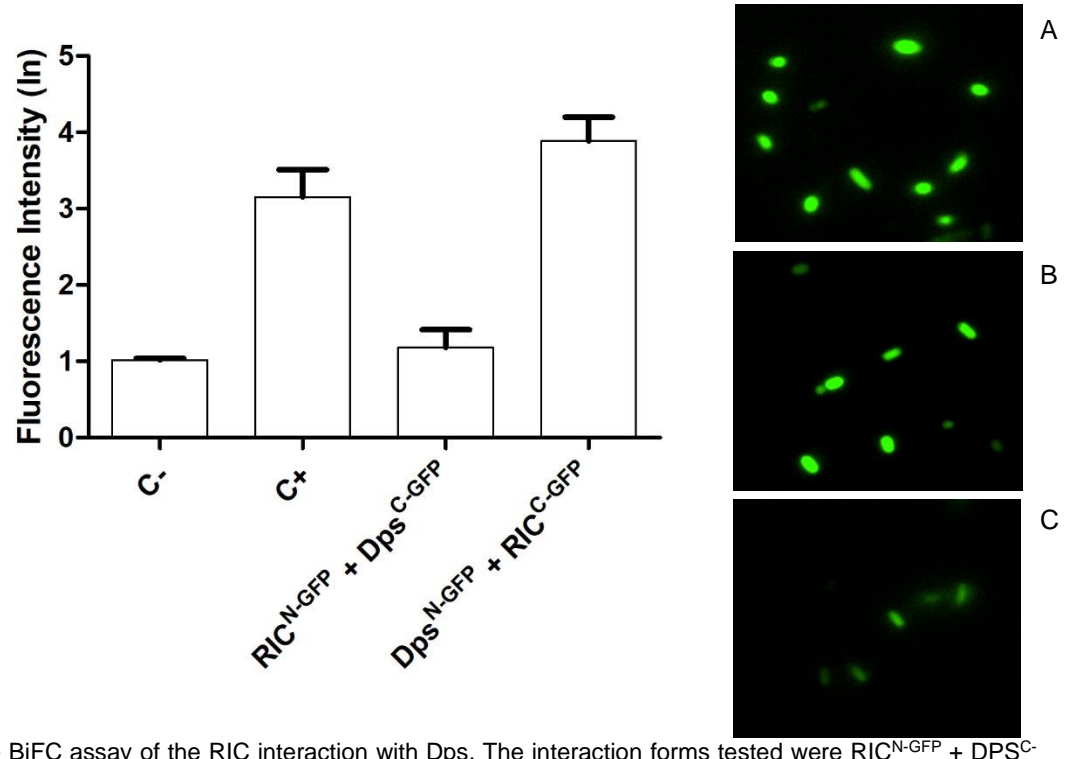


**Figure 4.18** - BiFC assay of the RIC interaction with Dps. The interaction forms tested were RIC<sup>N-GFP</sup> + DPS<sup>C-GFP</sup> and DPS<sup>N-GFP</sup> + RIC<sup>C-GFP</sup> interaction forms. The negative control pET11a-link-N-GFP and pMRBAD-link-C-GFP and pET11a-dps-N-GFP and pMRBAD-yftE-C-GFP as the positive. A - DPS<sup>N-GFP</sup> + RIC<sup>C-GFP</sup>. B -Positive Control. C – Negative control

Using the negative control (values normalized to 1) as a reference value, it is possible to verify that the positive control emits 3 times more fluorescence than the negative control. The RIC<sup>N-GFP</sup> + DPS<sup>C-GFP</sup> sample has a fluorescence very similar to the negative control whereas the DPS<sup>N-GFP</sup> + RIC<sup>C-GFP</sup> interaction has an intensity value higher than the positive control which indicates that the two proteins interact in this conformation.

As in tests carried out by the laboratory previously, it was possible to determine that the *S. aureus* RIC protein has a protective role against oxidative stress and *E. coli*'s RIC protein is more

effective in nitrosative stress rather than oxidative stress. In the literature, it is described that Dps interacts with RIC in detoxification processes of  $E.\ coli^{32}$  therefore this test tried to determine if there is a possibility that these proteins interact in  $S.\ aureus$ , and perhaps participate in detoxification mechanisms of reactive oxygen species.

BiFC allowed us to visualize, through fluorescence, that the conformation pET11a-Dps-N-GFP and pMRBAD-RIC-C-GFP interacts inside the cell. This intensifies the idea that RIC has a protective role in cells exposed to ROS (figure 4.18).

The interaction between these two proteins is crucial for cell survival, since in Dps deficiency RIC produces ROS<sup>32</sup>. This suggests that RIC releases iron to the cytoplasm that generates free radicals resulting in ROS formation.

## 4.5. Site-directed mutagenesis

In order to study the role of some conserved residues in the RIC protein, single or double mutations were made in residues of *S. aureus* RIC protein. The mutants were produced using primers with the intended mutations through PCR. With the amplified DNA, *E. coli* XL1 competent cells were transformed with the single mutated vector and *E. coli* XL10 competent cells with the double mutated vector.

To check which colonies were transformed, a colony PCR was performed (figure 4.19). All colonies tested presented a band in the region of ~750bp, corresponding to the size of the amplified gene.

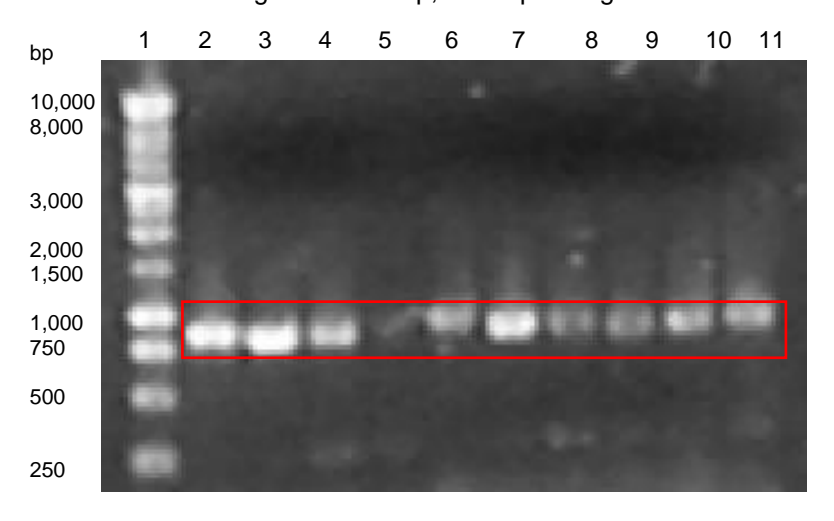


**Figure 4.19** - Colony PCR of the strains *E. coli* XL1 and XL10 in a 1% agarose gel. 1- ladder Promega 1Kb. 2 to 4 - single mutant AxxxE) 5 to 11 -doble mutant (GxxxE AxxxE).

To confirm whether the mutations were present, DNA was extracted from the corresponding colonies present in the wells 2 and 3 (single mutant AxxxE) and wells 9 and 10 (double mutant GxxxE AxxxE) and the pDNA was sequenced to confirm the mutations.

# 5. Conclusions

This project aimed to study in more detail the *S. aureus* RIC protein beyond its function of Fe-S repair and iron donor properties which had raised the possibility that *S. aureus* RIC might also have a catalase functionality.

In order to evaluate resistance and viability to stress conditions, JE2 and JE2 $\Delta$ ric strains were submitted to oxidative stress in their growth. In the oxidative stress assay, the mutant grew less than the WT therefore, the mutant is less resistant to hydrogen peroxide than WT. In addition to this, cell viability was also tested. These results demonstrate that over time, the cells remained viable, although, its viability was decreasing, despite not growing. Thus, indicating that the oxidative stress has a great impact in JE2 $\Delta$ ric cells viability and resistance.

Furthermore, through the analysis of the enzymatic activity of JE2 and JE2 $\Delta$ *ric* cell extracts, it was shown that RIC has a crucial role in protecting the cells from oxidative stress in the exponential phase compared to the stationary phase, since the activity of the mutant in the log phase has a decrease of 70% versus 9% in the stationary phase comparing to the WT strain.

The enzymatic activities of the complemented strain RIC and RIC C30AC31A achieved similar values to the WT activity, meaning that the complementation can restore the mutant phenotype.

Regarding RIC's interaction with Dps, it was determined that *S. aureus* RIC protein interacts with Dps like *E. coli*'s RIC protein. Since both proteins are highly conserved, this increases the relevance of RIC in its protective function against oxidative stress.

Looking into the activity and kinetic constants obtained in RIC purified protein, it is possible to conclude that the RIC protein itself does not function as a catalase. This result is also supported by the results obtained in the *E. coli* BW25113 *katE*, *katG* and *katEG* oxidative stress where the complemented mutants did not restored the phenotype.

In this thesis it was possible to conclude that RIC of *S. aureus* has a fundamental role in protecting the cells from oxidative stress through a possible involvement in a detoxifying mechanism rather than extra catalase function inside the cell.

# 6. References

- 1. Tosi, M. F. Innate immune responses to infection. *Journal of Allergy and Clinical Immunology* vol. 116 241–249 (2005).
- 2. Lim, D. & Strynadka, N. C. J. Structural basis for the β-lactam resistance of PBP2a from methicillin-resistant Staphylococcus aureus. *Nat. Struct. Biol.* **9**, 870–876 (2002).
- 3. Carrillo, J. L. M., Rodríguez, F. P. C., Coronado, O. G., García, M. A. M. & Cordero, J. F. C. Physiology and Pathology of Innate Immune Response Against Pathogens. *Physiology and Pathology of Immunology*. **6**, 99-134 (2017).
- 4. Reniere, M. L. Reduce, Induce, Thrive: Bacterial Redox Sensing during Pathogenesis. *J. Bacteriol.* **200**, (2018).
- Nobre, L. S., Meloni, D., Teixeira, M., Viscogliosi, E. & Saraiva, L. M. *Trichomonas vaginalis* Repair of Iron Centres Proteins: The Different Role of Two Paralogs. *Protist* 167, 222–233 (2016).
- 6. Justino, M. C., Vicente, J. B., Teixeira, M. & Saraiva, L. M. New genes implicated in the protection of anaerobically grown *Escherichia coli* against nitric oxide. *J. Biol. Chem.* **280**, 2636–2643 (2005).
- 7. Lo, F.-C. *et al.* Crystal Structure Analysis of the Repair of Iron Centers Protein YtfE and Its Interaction with NO. *Chem. A Eur. J.* **22**, 9768–9776 (2016).
- 8. Pisoschi, A. M. & Pop, A. The role of antioxidants in the chemistry of oxidative stress: A review. *European Journal of Medicinal Chemistry.* **97**, 55–74 (2015).
- Eid, R., Arab, N. T. T. & Greenwood, M. T. Iron mediated toxicity and programmed cell death:
   A review and a re-examination of existing paradigms. Biochimica et Biophysica Acta Molecular Cell Research. 1864, 399–430 (2017).
- Gnanamani, A., Hariharan, P. & Paul-Satyaseela, M. Staphylococcus aureus: Overview of Bacteriology, Clinical Diseases, Epidemiology, Antibiotic Resistance and Therapeutic Approach. in Frontiers in Staphylococcus aureus. 1, 3-28 (2017).
- 11. Hakim, L., Koga, K. & Tanaka, H. Thermodynamic stability of hydrogen hydrates of ice Ic and II structures. *Phys. Rev. B Condens. Matter Mater. Phys.* **82**, 1–11 (2010).
- 12. Lacey, K. A., Geoghegan, J. A. & McLoughlin, R. M. The role of *Staphylococcus aureus* virulence factors in skin infection and their potential as vaccine antigens. *Pathogens* **5** 1-17

(2016).

- 13. Kobayashi, S. D., Malachowa, N. & Deleo, F. R. Pathogenesis of Staphylococcus aureus abscesses. *American Journal of Pathology*. **185** 1518–1527 (2015).
- 14. Bradley, S. F. Staphylococcus. in *Clinical Infectious Disease*, 985–990 (2015).
- 15. Bien, J., Sokolova, O. & Bozko, P. Characterization of Virulence Factors of Staphylococcus aureus: Novel Function of Known Virulence Factors That Are Implicated in Activation of Airway Epithelial Proinflammatory Response. *J. Pathog.* **2011**, 1–13 (2011).
- 16. Chambers, H. F. & DeLeo, F. R. Waves of resistance: *Staphylococcus aureus* in the antibiotic era. *Nature Reviews Microbiology*. **7** 629–641 (2009).
- 17. Balasubramanian, D., Harper, L., Shopsin, B. & Torres, V. J. *Staphylococcus aureus* pathogenesis in diverse host environments. **75**, 5 (2017).
- 18. Fishovitz, J., Hermoso, J. A., Chang, M. & Mobashery, S. Penicillin-Binding Protein 2a of Methicillin-Resistant *Staphylococcus aureus*.
- 19. Foster, T. Staphylococcus. Medical Microbiology (1996).
- Guerra, F. E. et al. Staphylococcus aureus SaeR/S-regulated factors reduce human neutrophil reactive oxygen species production. J. Leukoc. Biol. 100, 1005–1010 (2016).
- 21. Liu, G. Y. Molecular Pathogenesis of *Staphylococcus aureus* Infection. *Pediatr. Res.* **65**, 71-77 (2009).
- 22. Feng, Y. *et al.* Evolution and pathogenesis of *Staphylococcus aureus*: lessons learned from genotyping and comparative genomics. *FEMS Microbiol. Rev.* **32**, 23–37 (2008).
- 23. Gaupp, R., Ledala, N. & Somerville, G. A. Staphylococcal response to oxidative stress. Frontiers in cellular and infection microbiology. **2**, 33 (2012).
- 24. Fontecave, M. Iron-sulfur clusters: Ever-expanding roles. *Nat. Chem. Biol.* **2**, 171–174 (2006).
- 25. Johnson, D. C., Dean, D. R., Smith, A. D. & Johnson, M. K. Structure, function, and formation of biological iron-sulfur clusters *Annu. Rev. Biochem.* **74**, 247-281(2005).
- Lu, Y. Assembly and transfer of iron–sulfur clusters in the plastid. Frontiers in Plant Science
   9, 336 (2018).
- 27. Rouault, T. A. Biogenesis of iron-sulfur clusters in mammalian cells: New insights and relevance to human disease. *DMM Disease Models and Mechanisms* **5**, 155–164 (2012).
- 28. Overton, T. W. et al. Widespread distribution in pathogenic bacteria of di-iron proteins that

- repair oxidative and nitrosative damage to iron-sulfur centers. *J. Bacteriol.* **190**, 2004–2013 (2008).
- Justino, M. C., Almeida, C. C., Gonçalves, V. L., Teixeira, M. & Saraiva, L. M. Escherichia coli YtfE is a di-iron protein with an important function in assembly of iron-sulphur clusters. *FEMS Microbiol. Lett.* 257, 278–284 (2006).
- 30. Roberts, C. A. *et al.* The Suf iron-sulfur cluster biosynthetic system is essential in *Staphylococcus aureus*, and decreased Suf function results in global metabolic defects and reduced survival in human neutrophils. *Infect. Immun.* **85**, 6 (2017).
- 31. Choby, J. E. *et al.* A Small-Molecule Inhibitor of Iron-Sulfur Cluster Assembly Uncovers a Link between Virulence Regulation and Metabolism in *Staphylococcus aureus*. *Cell Chem. Biol.* **23**, 1351–1361 (2016).
- Silva, L. S. O., Baptista, J. M., Batley, C., Andrews, S. C. & Saraiva, L. M. The di-iron RIC protein (YtfE) of *Escherichia coli* interacts with the DNA-binding protein from starved cells (Dps) to diminish RIC protein-mediated redox stress. *J. Bacteriol.* 200, e00527 (2018).
- 33. Nobre, L. S. *et al.* Insights into the structure of the diiron site of RIC from *Escherichia coli. FEBS Lett.* **589**, 426–431 (2015).
- 34. Silva, L. O., Nobre, L. S., Mil-Homens, D., Fialho, A. & Saraiva, L. M. Repair of Iron Centers RIC protein contributes to the virulence of *Staphylococcus aureus*. *Virulence*. **9** 312–317 (2018).
- 35. Karas, V. O., Westerlaken, I. & Meyer, A. S. The DNA-binding protein from starved cells (Dps) utilizes dual functions to defend cells against multiple stresses. *J. Bacteriol.* **197**, 3206–3215 (2015).
- Nobre, L. S. et al. Escherichia coli RIC Is Able to Donate Iron to Iron-Sulfur Clusters. PLoS One 9, e95222 (2014).
- 37. Mammina, C. *et al.* Polyclonal non multiresistant methicillin resistant *Staphylococcus aureus* isolates from clinical cases of infection occurring in Palermo, Italy, during a one-year surveillance period. *Ann. Clin. Microbiol. Antimicrob.* **11**, 17 (2012).
- 38. Bose, J. L., Fey, P. D. & Bayles, K. W. Genetic tools to enhance the study of gene function and regulation in Staphylococcus aureus. *Appl. Environ. Microbiol.* **79**, 2218–2224 (2013).
- 39. Vine, C. E., Justino, M. C., Saraiva, L. M. & Cole, J. Detection by whole genome microarrays of a spontaneous 126-gene deletion during construction of a *ytfE* mutant: confirmation that a *ytfE* mutation results in loss of repair of iron-sulfur centres in proteins damaged by oxidative

- or nitrosative stress. J. Microbiol. Methods 81, 77-79 (2010).
- 40. Hazan, R., Que, Y.-A., Maura, D. & Rahme, L. G. A method for high throughput determination of viable bacteria cell counts in 96-well plates. *BMC Microbiology*. **12**, 259 (2012)
- 41. Bisswanger, H. Enzyme assays. *Perspect. Sci.* **1**, 41–55 (2014).
- 42. Schnell, S. Validity of the Michaelis-Menten equation Steady-state or reactant stationary assumption: That is the question. *FEBS J.* **281**, 464–472 (2014).
- 43. Wilson, C. G. M., Magliery, T. J. & Regan, L. Detecting protein-protein interactions with GFP-fragment reassembly. *Nat. Methods* **1**, 255–262 (2004).
- 44. Bachman, J. Site-Directed Mutagenesis. *Methods in enzymology.* **529**, 241–248 (2013).
- 45. Arkin, M. In vitro Mutagenesis. in Encyclopedia of Genetics. 200, 1010–1014 (2001)...
- 46. Walker, K. W. Site-Directed Mutagenesis. in *Encyclopedia of Cell Biology*. 1 1 122–127 (2016).
- 47. Mashruwala, A. A. & Boyd, J. M. The *Staphylococcus aureus* SrrAB Regulatory System Modulates Hydrogen Peroxide Resistance Factors, Which Imparts Protection to Aconitase during Aerobic Growth. *PLoS One* **12**, 1 (2017).
- 48. Hughes, K. Complementation. *Brenner's Encyclopedia of Genetics: Second Edition* 111–112 (2013).
- 49. Lo, F.-C. *et al.* Crystal Structure Analysis of the Repair of Iron Centers Protein YtfE and Its Interaction with NO. *Chem. A Eur. J.* **22**, 9768–9776 (2016).
- 50. Bertoldo, J. B. *et al.* A Water-Bridged Cysteine-Cysteine Redox Regulation Mechanism in Bacterial Protein Tyrosine Phosphatases. *Chem* **3**, 665–677 (2017).
- 51. Chauvatcharin, N., Vattanaviboon, P., Switala, J., Loewen, P. C. & Mongkolsuk, S. Cloning and characterization of *katA*, encoding the major monofunctional catalase from Xanthomonas campestris pv. phaseoli and characterization of the encoded catalase *katA*. *Curr. Microbiol.* **46**, 83–87 (2003).
- 52. Panek, H. R. & O'Brian, M. R. KatG is the primary detoxifier of hydrogen peroxide produced by aerobic metabolism in *Bradyrhizobium japonicum*. *J. Bacteriol.* **186**, 7874–7880 (2004).
- 53. Iwase, T. *et al.* A simple assay for measuring catalase activity: A visual approach. *Sci. Rep.* **3**, 1–4 (2013).
- 54. De La Fuente, R., Díez, R. M., Domínguez-Bernal, G., Orden, J. A. & Martínez-Pulgarín, S. Restoring catalase activity in *Staphylococcus aureus* subsp. anaerobius leads to loss of pathogenicity for lambs. *Vet. Res.* **41**, 4 (2010).

# S. Supplements

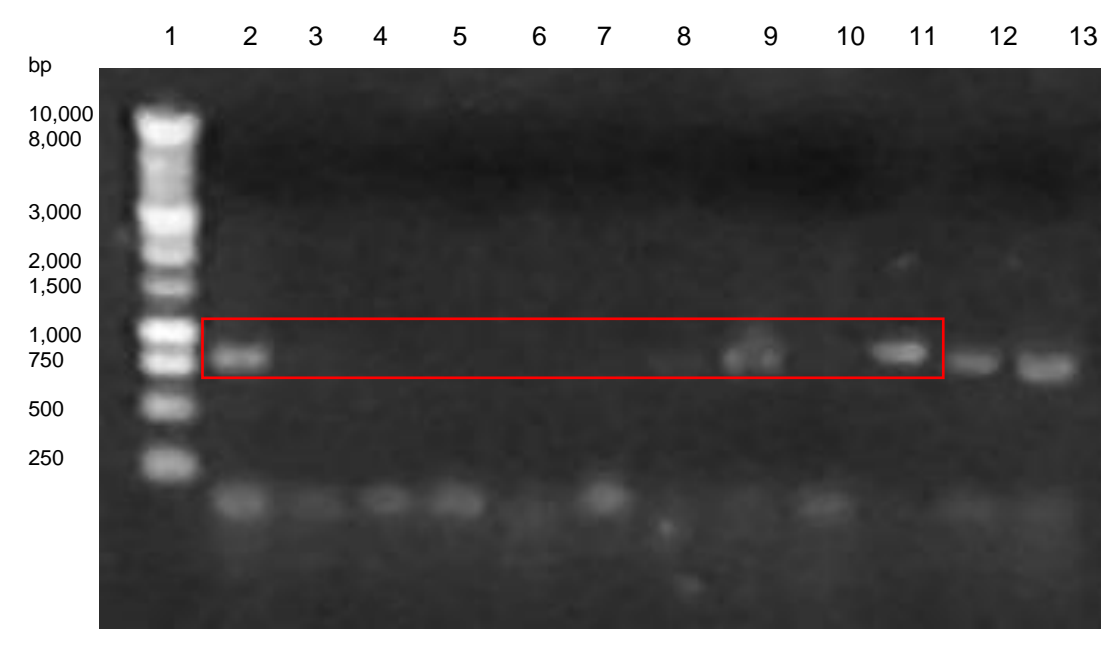


**Figure S.1.** – A 1% agarose gel exemplifying and colony PCR of *E. coli* XL1. RIC samples are presented in lanes 2 to 10 and RIC C30AC31A in lanes 11 to 13. The ladder is in the first well.

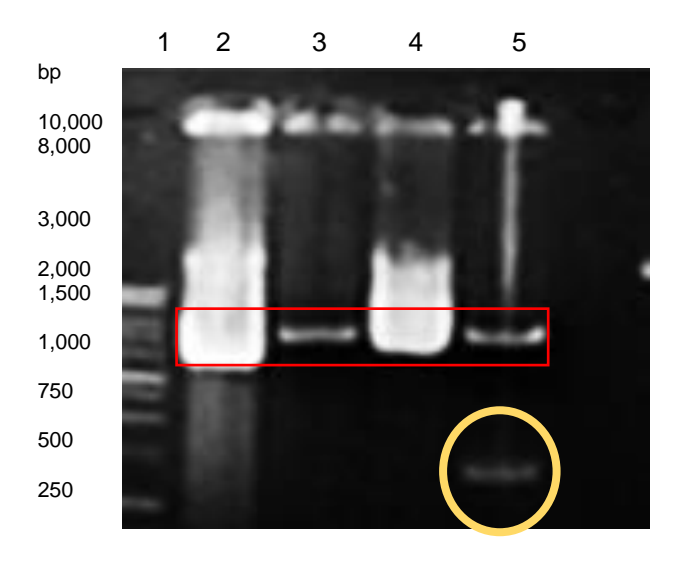


**Figure S.2** – Digestion of pMK4 plasmid. 1% agarose 1% gel containing the pDNA *S. aureus* RN4220 digested (lanes 3 and 5) and non-digested (lanes 2 and 4). Wells 1-marker Promega 1Kb 2- pMK4 non-digested; 3 - pMK4 digested; 4 - pMK4-RIC non-digested; 5 - pMK4-RIC digested.

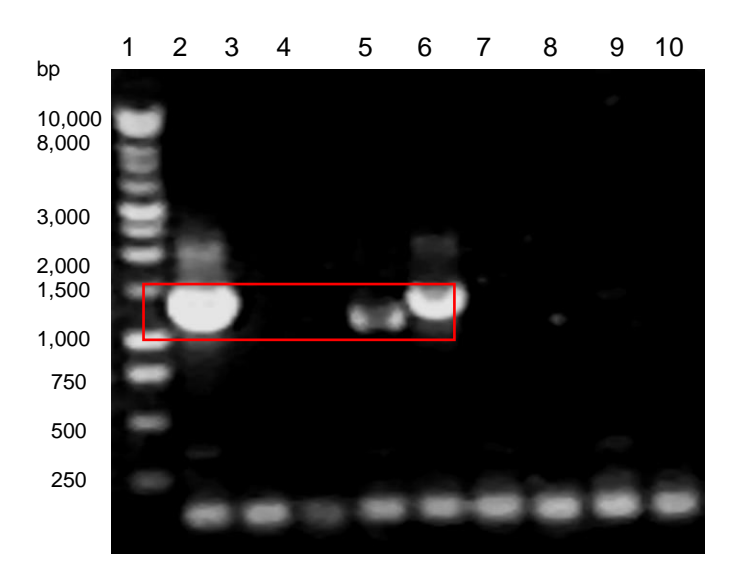


**Figure S.3** – Transformation of JE2 $\Delta ric$  with pMK4 and pMK4-RIC for the complementation activity assays. A 1% agarose gel exemplifying a JE2 $\Delta ric$  pMK4 and pMK4-RIC colony PCR. Lane 1 – Maker, lanes 2-6 pMK4-RIC, lanes 7-10 pMK4.

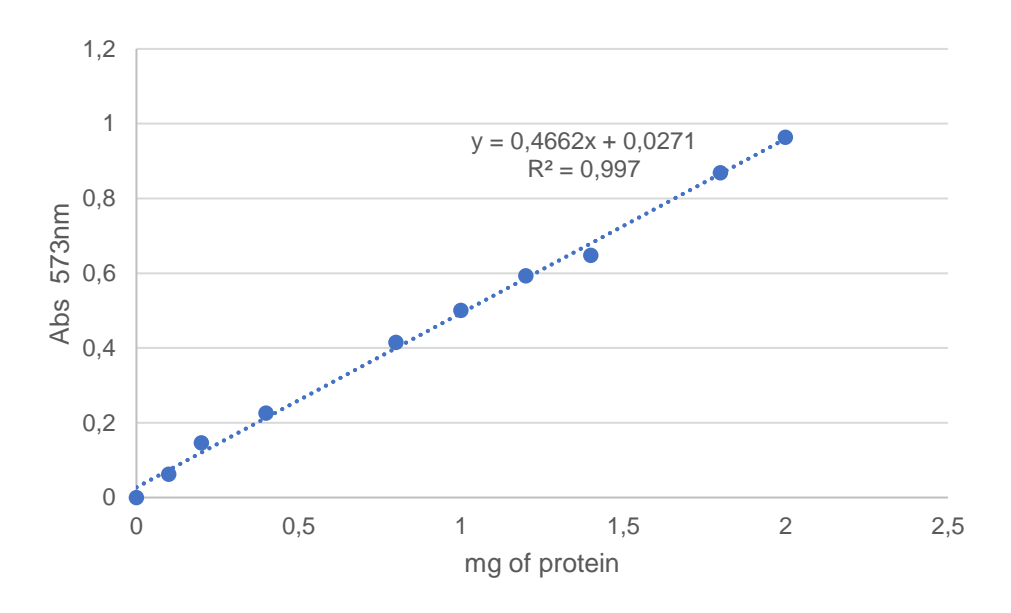


**Figure S.4 –** BCA calibration curve used to quantify the mg of protein present in the cell lysates and purified protein. The standard used was BSA.

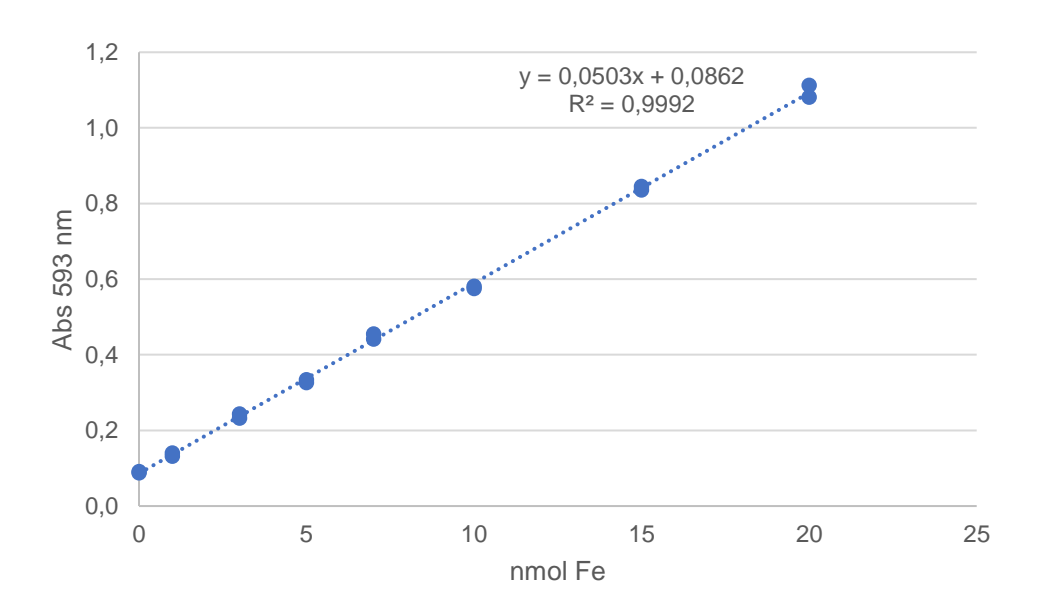


**Figure S.5 –** TPTZ calibration curve used in the RIC protein iron quantification.